Dear editor,

in the revision of our paper *"3D Shear layer simulation model for the mutual interaction of wind turbine wakes: Description and first assessment"*, we followed the suggestions by the referees and addressed their comments point to point in two separate documents. Inspired by the reviews, we developed our model further and added additional content to make the evaluation of the model comprehensive. In particular:

- We enhanced the method to initialise the far wake and deal with the near wake following the approach applied in other shear layer engineering wake models. [Werle, 2015, Madsen et al., 2010].
- We refined and at the same time simplified the eddy viscosity model using an analytical wake model [Frandsen et al., 2006, Rathmann et al., 2006] to estimate the turbulent mixing length with the wake radius.
- We improved the model of the ambient eddy viscosity which now varies with the height instead of having a fixed value defined by the wind turbine hub height.
- We used the Ainslie model as implemented in the wind farm layout software *FLaP* [Lange et al., 2003], instead of using the three dimensional shear layer model (3DSL) to simulate the single wakes used in the square addition approach.
- We included two additional methods of evaluation for the shear layer models, namely the root mean square error and the regression analysis, both in relation to the wakes of the reference large eddy simulation wind fields.
- We considered four test cases including single and multiple wakes. We also generalised the title accordingly: *3D Shear layer model for the simulation of multiple wind turbine wakes: Description and first assessment.*

The new results show that our model is at least equivalent and sometimes more accurate than the Ainslie model implemented in *FLaP* in the test cases analysed. In this sense, the paper indicates that our model works and its innovations are worth to be further investigated.

We hope in your positive evaluation of the revised version of our paper and thank you for the efforts you and the referees spent for the review process.

Best regards,
Davide Trabucchi on behalf of all the authors

References

S. Frandsen, R. Barthelmie, S. Pryor, O. Rathmann, S. Larsen, J. Højstrup, and M. Thøgersen. Analytical modelling of wind speed deficit in large offshore wind farms. *Wind Energy*, 9(1-2):39–53, 2006. ISSN 1099-1824. doi: 10.1002/we.189.

B. Lange, H.-P. Waldl, A. G. Guerrero, D. Heinemann, and R. J. Barthelmie. Modelling of offshore wind turbine wakes with the wind farm program flap. *Wind Energy*, 6(1):87–104, 2003. ISSN 1099-1824. doi: 10.1002/we.84.

H. A. Madsen, G. C. Larsen, T. J. Larsen, N. Troldborg, and R. Mikkelsen. Calibration and validation of the dynamic wake meandering model for implementation in an aeroelastic code. *Journal of Solar Energy Engineering*, 132(4):041014–041014, Oct. 2010. ISSN 0199-6231. doi: 10.1115/1.4002555.

O. Rathmann, R. Barthelmie, and S. Frandsen. Turbine wake model for wind resource software. In *EWEC*, 2006. URL `https://www.researchgate.net/profile/R`$_B arthelmie/publication/268300272_T urbine_W ake_M odel_f or_W ind_R esource$ $0pdfJsDownload = 0origin = publication_d etail$.

M. J. Werle. Another engineering wake model variant for horizontal axis wind turbines. *Wind Energy*, pages 279–299, 2015. ISSN 1099-1824. doi: 10.1002/we.1832. WE-14-0059.R2.

Response to the first referee's review of the paper *"3D Shear layer simulation model for the mutual interaction of wind turbine wakes: Description and first assessment"*

Davide Trabucchi, Lukas Vollmer and Martin Kühn

General comment

This paper concerns a new shear layer simulation model to predict multiple wake interactions. The suggested model can be considered as an extended version of the model originally developed by Ainslie, 1988. In its original form of the model, steady-state RANS equations are written in a cylindrical form with an assumption that the flow is axisymmetric. As a consequence, the model was not able to quantify the flow if turbines are not located in a row. To overcome this limitation, the authors in the current study developed a new model by writing the governing equations in a Cartesian coordinate so that the model is basically able to predict wake interactions if turbines are placed in a random manner (not necessarily in a row).

The authors stated the main motivation of this work as the fact that the superimposition (e.g., sum of squares) of single wakes, predicted by existing engineering models, is not supported by a physical background. I agree with the authors that physical interpretation of different superimposition methods (e.g., sum of square, linear sum of velocity deficit) is far from being well understood and more research should be performed in this context.

However, I do not believe that this work can overcome this limitations because it is based on several assumptions that question the universality of this work. For instance, the model is quite complicated, with respect to simple analytical models, due to the inclusion of several different parameters to estimate the turbulent viscosity and then the flow field in the far wake region.

However, at the end, the model predictions do significantly depend on near-wake characteristics, which are fed into the model as boundary conditions. The bottle neck here is the fact that, as far as I understood, the near wake length is simply assumed to be 2 rotor diameter regardless of incoming flow and turbine characteristics which is a very questionable assumption. Moreover, the magnitude of the velocity at the end of the near wake is based on Betz theory.

In other words, this study makes the far-wake simulation much more sophisticated but model predictions still depend on very basic and questionable assumptions for the near-wake region.

I have some other major concerns about the development and validation of the model, listed below. Overall, I believe that the paper is not suitable for publication in Wind Energy Science (WES) within its current form.

Reply: The main criticism by the reviewer is that the assumption in the formulation of new model and the simple method applied to estimate its initial condition prevent the model from the possibility to improve the simulation of interacting wakes. To verify this, in the revision of the paper, we decided to compare the three dimensional shear layer model (3DSL) to the Ainslie model applied to single and multiple wakes, instead of applying superposition rules to the 3DSL

itself. So,the comparison is more general and it also evaluates the 3DSL model directly and not only in relation to the superposition of multiple wakes. As in the first version of the paper, we used LES including wakes as reference for the evaluation of the accuracy of the two models.

The results show that actually the three dimensional shear layer model can deal better than the square addition approach applied to the Ainslie model in the cases analysed. We do not believe that the superposition of multiple wakes is the only reason for the different results. However, we think that a relatively simple three dimensional model broadens up the possibility for improvement and further developments.

Concerning the problem of the initial conditions we changed our approach to avoid the direct imposition of a wake deficit at a fixed downstream distance; about the eddy-viscosity model we simplified its formulation with the support of an analytical wake model.

Major comments

- In general, the way that the results of "wake interaction" and "square addition" are compared with the LES data is not appropriate and needs major modifications. The main criticism here is that the predictions of 3DSL are used in both cases but model predictions might be inaccurate even for the wake of a single turbine. In fact, figure 8.a shows that "wake addition" method largely overestimates the velocity even for $x = 10\,D$ at $y > 0$, where the effect of the first turbine is only seen (see figure 6). Therefore, the error can be due to inaccurate predictions of a single wake rather than the sum-of-square approach. Having this in mind, comparison of the 3DSL simulation with the LES data for the wake of a single turbine is useful and should be added to the manuscript.

  Reply: We followed the suggestion and we considered a single wake in our study too. The results are included in Section 3.3.1 of the manuscript.

- Figure 8.a: Following the above comment, I expect to see identical results for both "wake interaction" and "wake addition" methods if there is only the effect of a single wake. However, the results shown in the above panel of figure 8.a do not support this! Please explain the reason.

  Reply: This comment does not apply anymore to the revised version of the manuscript.

- It is a well-known fact that near wake length depends on several parameters such as the turbulence intensity of the incoming flow as well as turbine characteristics. As mentioned earlier, the use of a constant value (2 rotor diameters) for the near wake length for all the turbines questions the validity of the whole simulation.

  Reply: In the first version of the paper we followed the example by Ainslie [1988], who indicates the length of the near wake to be about 2 D. In the new revision, we opted for the approach introduced by Madsen et al. [2010] to solve the flow in the dynamic wake meandering model (DWM). It consists in a two steps method for the calculation of the initial conditions of the wake: First it computes the deficit at the outlet of the induction zone, then it lets the wake deficit develop under the influence of the turbulent mixing, starting from the rotor cross-section. At the same time, it applies an additional filter to the eddy viscosity with the scope of reducing the diffusion in the near wake region. The range

in which the filter is applied is still a fixed parameter, but this solution is not as strong as imposing a specific deficit at a fixed downstream distance. A similar approach is applied by Werle [2015] too.

- The justification for the use of a fixed turbulence mixing length is quite poor. Although this assumption leads to results that are in agreement with the LES data, it is not based on any physical evidence.

  Reply: In the revision of the paper, we evaluated the radius of the wake with the analytical model by Frandsen et al. [2006] and revised by Rathmann et al. [2006]. The closest upstream turbine is considered to define the turbulence mixing length where multiple wakes are overlapping. Other equivalent models could be used for the same purpose.

- Please elaborate how the function $g(y, z)$ is determined.

  Reply: $g(y, z)$ is just a help function used to rename the streamwise gradient of u_D. This gradient is evaluated from the known values of u_D, v, w at the previous step applying a central finite difference scheme.

- The assumption that the lateral and vertical velocities can be expressed as derivatives of a potential function is poorly justified. This assumption implies that the vorticity in the streamwise direction is equal to zero. The authors need to provide more physical explanation to prove the validity of this assumption.

  Reply: The assumption of a potential flow on the vertical cross-section is implicit in common shear layer axisymmetric wake models since they resolve only the streamwise and radial wind components, i.e. the flow has no tangential velocity. In our work we deal with a model which belongs to the same category. Our extension drops the assumption of an axialsimmetric flow and allows to find one of the possible solutions of the underdeterminated three dimensional shear layer problem. This solution satisfies the conservation of the mass and is in accordance with the approximated equation of the momentum balance in the streamwise direction. Furthermore, some wake vortex models assume a conservative flow almost on all the simulation domain. We elaborated on this topic in Sect. 2.1 (page 4, from line 9).

- Page 5, line 24: Please plot the variation of wake radius as a function of downwind location. Wake radius is defined in this paper as the distance between the wake center and where the wake velocity deficit is 0.1%. Why is this value selected? Some other definitions for the wake width such as the standard deviation of a Gaussian curve fitted to velocity deficit profiles can be used.

  Reply: The radius is now defined according to the analytical model by Frandsen et al. [2006] and revised by Rathmann et al. [2006] (see Sect. 2.4.1, page 8 from line7). We included the corresponding formulation, but no plot.

- Page 6, line 19: The iteration process to estimate the value of D_i is unclear. If the value of C_T is known then the induction factor and consequently D_i can be easily obtained and no iterative process is needed. Please clarify it.

  Reply: The point here is that C_T depends on the inflow velocity $U_{RE,i}$ which is dependent on D_i. Since the latter depends on C_T to satisfy the conservation of mass, an iterative

process is needed. We extended the corresponding paragraphs in section 2.3 to explain in a more clear way the need of the iteration (see page 6, from line 17).

- Page 7, line 8: I agree that within wind farms, the estimation of the incoming velocity is not a very straightforward task as the velocity changes with the streamwise position. However, the flow on the rotor plane cannot be considered as the incoming flow since the flow velocity at the rotor is definitely smaller than the one of the incoming flow due to the induction flow region upwind of the turbine. Instead, I think you should consider the flow on the rotor as the incoming flow divided by (1-a).

  Reply: This is a very delicate matter for which an accurate induction model within wakes would be required. Here, we chose a practical solution similar to the approach of the ECN model implemented in WakeFarm and explained in chapter 9.5.4 of [Schepers, 2012]. Since we cannot consider the speed up given by the recovery of the wake and at the same time the deceleration due to the induction of the rotor, we had to chose between one of the two phenomena. In this regard, we decided to compress the induction zone into an infinitesimally long stream tube at the rotor cross section. In this stream tube flow is decelerated and expanded according to the disk actuator model.

- Equation 18: Sum-of-squares superposition is one of the approaches used in the literature. For instance, Niayifar and Porté-Agel (2015) showed that velocity deficit superposition provides more realistic results if the wake growth rate is adjusted based on the value of turbulence intensity in a wind farm. The results based on velocity deficit superposition can be added for the sake of comparison.

  Reply: We performed a comparison of the two models also for the linear addition approach, but we chose not to report the results because the square addition approach provided in general better results and a comparison of both approaches is out of the scope of this research.

- Equation 2: The first terms in the continuity and x-RANS equations are divided by u_i , while other terms are not.

  Reply: v and w are also normalised dividing by a reference wind speed. The inaccurate definition of the equation has been corrected.

References

F. Ainslie, J. Calculating the flowfield in the wake of wind turbines. *Journal of Wind Engineering and Industrial Aerodynamics*, 27:213–224, 1988. doi: 10.1016/0167-6105(88)90037-2.

S. Frandsen, R. Barthelmie, S. Pryor, O. Rathmann, S. Larsen, J. Højstrup, and M. Thøgersen. Analytical modelling of wind speed deficit in large offshore wind farms. *Wind Energy*, 9(1-2): 39–53, 2006. ISSN 1099-1824. doi: 10.1002/we.189.

H. A. Madsen, G. C. Larsen, T. J. Larsen, N. Troldborg, and R. Mikkelsen. Calibration and validation of the dynamic wake meandering model for implementation in an aeroelastic code. *Journal of Solar Energy Engineering*, 132(4):041014–041014, Oct. 2010. ISSN 0199-6231. doi: 10.1115/1.4002555.

O. Rathmann, R. Barthelmie, and S. Frandsen. Turbine wake model for wind resource software. In *EWEC*, 2006. URL https://www.researchgate.net/profile/R$_B$*arthelmie*/*publication*/268300272$_T$*urbine*$_W$*ake*$_M$*odel*$_f$*or*$_W$*i* 0*pdf JsDownload* = 0*origin* = *publication*$_d$*etail*.

G. Schepers, Jan. *Engineering models in wind energy aerodynamics. Development, implementation and analysis using dedicated aerodynamic measurements*. PhD thesis, ECN, 2012.

M. J. Werle. Another engineering wake model variant for horizontal axis wind turbines. *Wind Energy*, pages 279–299, 2015. ISSN 1099-1824. doi: 10.1002/we.1832. WE-14-0059.R2.

Response to the second referee's review of the paper *"3D Shear layer simulation model for the mutual interaction of wind turbine wakes: Description and first assessment"*

Davide Trabucchi, Lukas Vollmer and Martin Kühn

General comment

The authors present an extension of the Ainslie wake model, which account for non-axisymmetric wake shapes and includes explicit (rather than assumed) wake-wake interactions. This is an important step towards an intermediary between existing engineering models and CFD. However, the paper has some shortcomings in presentation and in content.

I miss a description of the evolution of the wake shape in the new model. What does the wake cross section look like in the near wake? Figure 7 shows this in the far wake, but it would be useful with a line plot of the deficit profile in the cross stream or vertical direction at several downstream distances.

The comparison with FLaP in the case of an axisymmetric wake does not add anything significant to the manuscript. For a single, axisymmetric wake the equations reduce essentially to the Ainslie model, and section 3.1.1 is akin to a verification of the numerical scheme against another numerical implementation. It is nice to know that this has been done, but the details can be omitted from the paper.

In my view the paper presents a novel idea, which has the potential to move engineering wake models forward. The weak part of the model in its present state is the near wake model, which is taken directly from FLaP/Ainslie. The authors ought to have critically addressed the near wake formulation, which is overly complicated with a great number of constants and parameters, yet seem responsible for much of the difference between the model and the reference field.

The paper is publishable in its present form, but can be improved with further work. At the very least the authors should adopt the turbulence mixing model introduced at the end, almost as an afterthought, from the beginning of the paper instead.

Reply: Thank you for the comments and suggestions regarding the paper. With our work, we initially aimed to present a new model for the simulation of the mutual wake interaction outside the induction zone downstream of the wind turbine rotors. For this reason, the main focus was more on the solution of the shear layer approximation of the steady Reynolds Averaged Navier Stokes equations for non-axisymmetric wakes than on the development of accurate near wake or eddy viscosity models.

In the revised paper, we improved the near wake model following an approach more sophisticated but still easy to apply which is also implemented in other engineering wake models. Furthermore, we considered the radius of the wake as turbulent mixing length. For this purpose we used an analytical wake model.

As suggested we removed the direct comparison of the wake radius and center line deficit estimated from the 3DSL model and the FLaP simulations. Instead we included four test cases reproducing single and multiple wakes. In all these test cases we compared the 3DSL model with the square addition method applied to FLaP simulations of individual wakes and used LES wind fields including wakes as reference. Some of the corresponding horizontal and vertical profiles of the wake deficit are included in an appendix.

Major comments

- Add a description of the simulation time for a single wind speed and direction inflow case at least for the three-WTG example given. It is an important aspect in adopting a new model to understand how practical it is from an operational point of view and how much investment is needed in terms of coding.

  Reply: We included this piece of information in Sect. 3.2 (page 10 lines 5 and 12).

- P 4, line 18: can you be more specific on how the downstream step size is evaluated at each cross section? It would help a reader who desired to implement the model and work on refining it.

  Reply: Section 2.2 was extended including more details about the numerical implementation of the model and about the downstream step in relation to numerical stability (page 5, from line 10).

- P 5, equation (8): $(x - 4.5)^{1/3}$ becomes complex for $x > 4.5$. Are the limits $x >< 5.5D$ meant to be at $4.5D$? If not, then specify in the text how you handle the complex values in $F(x)$, or better re-write the equation so it is clear mathematically. For example, if you end up just taking the real part.

  Reply: The limits in the paper are correct. In equation (8), with $(x - 4.5)^{1/3}$ we intended the real cube root of $(x - 4.5)$. We added a footnote on page 7 to clarify this issue.

- P5, lines 21-24: are the characteristic turbulence length scales r_y and r_z updated at each vertical cross-section as the wakes are propagated forward? A drawing would help make the calculation of r_y and r_z easier to understand – illustrating the averaging of all deficits corresponding to the same y(z) and finding the width.

  Reply: We simplified the evaluation of the characteristic turbulence length scales and do not apply this method anymore.

- P6, line 11: the REWS concept has a specific meaning in the literature on power curves, where it signifies the cubic root of the average kinetic energy flux over the rotor. This is not the same as the average wind speed on the rotor plane. If you do mean the REWS in the power curve sense, then please include a reference to Wagner et al, Wind Energy 8, 993 (2011) at this point and rephrase the parenthesis at the end of line 11 (or replace it with a formal definition in an equation). If you meant instead the arithmetic mean of the wind speed on the rotor plane, then please use a different notation than REWS throughout the manuscript.

Reply: We agree with the reviewer that the definition of the rotor equivalent wind speed was not accurate in the paper. In the revision we decided to use the rotor average wind speed instead of the rotor equivalent wind speed.

- P 6, equation (13): please provide a reference for this equation.

  Reply: Equation (13) is derived from the actuator disc concept as explained for instance in section 3.2 of [Burton et al., 2011].

- P6, equation (16): include a reference to Figure 2, when discussing the stream tubes.

  Reply: We implemented this suggestion in the revision of the paper.

- P7: add more reasoning for breaking the calculation into blocks. What is the purpose or what problem does this approach solve?

  Reply: The simulation needs to be broken down in blocks because the wakes of the downstream wind turbines need to be considered sequentially. This practical detail is not relevant anymore. It was included in the paper to explain how the turbulence length scales developed across the simulation domain. With the new formulation of the turbulence length scales model, the concept of the blocks is no more relevant.

- P7: in the description of how the simulation is divided into blocks, a drawing would help the reader and make the conceptual structure of the calculations clearer.

  Reply: The blocks of simulations are not addressed in the paper anymore.

References

T. Burton, N. Jenkins, D. Sharpe, and E. Bossanyi. *Wind Energy Handbook, 2nd Edition*. John Wiley & Sons, Ltd., Publication, 2011.

3D Shear layer ~~simulation~~ model for the ~~mutual interaction~~ simulation of multiple wind turbine wakes: Description and first assessment

Davide Trabucchi, Lukas Vollmer, and Martin Kühn

ForWind - University of Oldenburg, Institute of Physics, Küpkersweg, 70, 26129 Oldenburg, Germany

Correspondence to: Davide Trabucchi (davide.trabucchi@uni-oldenburg.de)

Abstract. The number of turbines installed in offshore wind farms has strongly increased in the last years and at the same time the need for more precise estimation of the wind farm efficiency too. In this sense, the interaction between wakes has become a relevant aspect for the definition of a wind farm layout, for the assessment of its annual energy yield and for the evaluation of wind turbine fatigue loads. For this reason, accurate models for multiple wakes are a main concern of the wind energy community. Existing engineering models can only simulate single wakes which are superimposed when they are interacting in a wind farm. This method is a practical solution, but it is not fully supported by a physical background. The limitation to single wakes is given by the assumption that the wake is axisymmetric. As alternative, we propose a new shear layer model which is based on the existing engineering wake models, but is extended to simulate also non-axisymmetric wakes. In this paper, we present the theoretical background of the model and ~~two~~ four application cases. ~~First, we proved that for axisymmetric wakes the new model is equivalent to a commonly used engineering model. Then, we evaluated the improvements of~~ We evaluate the new model for the simulation of single and multiple wakes using large eddy simulations as reference. In particular, we report the improvements of the new model predictions in comparison to a sum-of-squares superposition approach for the simulation of three interacting wakes. ~~The remarkable~~ The lower deviation from the reference ~~in terms of rotor equivalent wind speed considering two and three interacting~~ considering single and multiple wakes encourages the further development of the model ~~,~~ and promises a successful application for the simulation of wind farms.

1 Introduction

When the wind passes through the wind turbine rotor, kinetic energy is extracted from the wind and is converted into electrical power. ~~This process generates a wake which propagates downstream.Wakes can be described as shear flows~~ The reduced kinetic energy is revealed by a wake deficit behind the rotor, i.e. a shear flow with lower speed and higher turbulent fluctuations than in ~~front of the rotor.~~ the free flow upstream and sideways.

In this sense, wakes are the main cause of power losses in wind farms (Walker et al., 2016). Besides that, wakes hitting a turbine contribute to the increase in the fatigue loads of its components. For these reasons, wake modeling plays a major role in the definition of the layout of wind farms, in the evaluation of their annual energy yield and in the estimation of the lifetime of

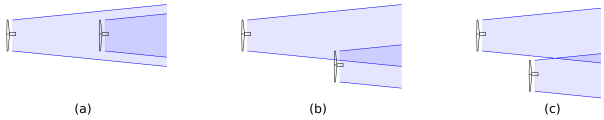

Figure 1. Different cases of merging wakes: (a) Aligned wakes (b) Wake-turbine interaction (c) Wake-wake interaction.

wind turbine components. Consequently, more accurate wake models can indirectly contribute to the cost-of-energy reduction ~~due~~ thanks to more tailored design of wind turbines and wind farms.

Despite the large progress especially in the numerical modelling, Vermeer et al. (2003) still provide a comprehensive review about traditional wake modeling. Most of the engineering models described in their work evaluate the wind field of a single wake and combine the individual results in case of mutual interaction. More sophisticated Computational Fluid Dynamics (CFD) such as Reynolds ~~Average~~ averaged Navier-Stokes (RANS) or ~~Large Eddy Simulations~~ large eddy simulations (LES) can ~~deal with wake superposition better and~~ provide more realistic results because the physics of the flow is resolved up to more refined length and time scales. However, these alternatives have a much higher computational cost and therefore can become prohibitive for ~~commercial~~ design applications.

~~Commercial codes~~ Engineering tools for estimating wake effects in a wind farm often implement the steady state, axisymmetric shear layer approximation of the RANS equations, e.g. the one used in the Ainslie model (Ainslie, 1988). Due to the axial symmetry assumption, only the wind deficit of single wakes or wakes aligned on the same axis as those illustrated in Fig. 1a can be simulated with such models. For the case of wake-turbine or wake-wake interaction of Fig. 1b and c pragmatic methods are required. In the kinematic model by Katic et al. (1986), the square addition of the individual wake deficits is applied to ~~overcome this limitation and to be able to~~ deal with multiple wakes. In a previous study, Lissaman (1979) proposed ~~their linear addition~~ the linear addition of the wake deficits, however this method tends to overestimate the velocity deficit and could lead to unrealistic flow reversal when many wakes merge.

Machefaux (2015) compared the performance of the linear approach with the one of the square wake addition approach and noticed that the former is to be preferred for wakes of turbines operating at a low thrust coefficients, while the latter returns better results in the opposite case. From this observation, he developed a wake superposition model which combines the linear and square addition of single wakes using a weighted average depending on the thrust on the rotor.

Crespo et al. (1999) declared that the classical wake superposition methods ~~does~~ do not rely on a physical background and, if not handled properly, could lead to unrealistic results. This statement gives the motivation of this paper. ~~Herewith~~In this regard, we aim to ~~describe the~~ investigate whether a more detailed physical model could improve the simulation of multiple wakes. For this purpose, we picked up the suggestion by Ainslie (1988) to extend his model to the third dimension, dropping the hypothesis of an axisymmetric wake profile; accordingly, we developed the 3D shear layer (3DSL~~) model, that is an innovative engineering model able to deal with the superposition of wakes and based on physical principles without relying on an addition method. Moreover, this study aims to verify the consistency of the model with other axisymmetric models. Finally, the performances of the single wakes~~) model and tested its performances in relation to Ainslie's model and the square addition approach~~and of the~~

~~direct simulation of interacting wakeswith the 3DSL model are assessed against~~ . For the assessment, we addressed four cases including a single wake, aligned wakes, wake-turbine and wake-wake interaction; we used the wind fields extracted from ~~the~~ LES of the same wake conditions ~~. The rotor equivalent wind speed (REWS) is the figure of meritof the assessment~~as reference and considered the section average wind speed and the root mean square error as figures of merit.

2 Model description

In the following the theoretical background of the 3DSL model is provided along with the description of its numerical implementation. Moreover, it is explained how to evaluate the parameters needed to apply the model.

2.1 The mathematical definition

The 3DSL model ~~implements a~~ is meant to add the third dimension to the shear layer approximation of the steady RANS equations ~~following the approach described by Lange et al. (2003). It~~ for wind turbine wake simulations first described by Ainslie (1988), maintaining all his assumptions but the one of an axisymmetric wake profile. The 3DSL model is intended to ~~model~~ simulate the downstream development of the wind turbine wake deficit u_D defined as

$$u_D(x,y,z) = \frac{u_w}{u_i} 1 - \frac{u_i(z) - u(x,y,z)}{u_H} \tag{1}$$

using the inflow wind speed u_i~~and the wake wind speed u_w~~, the corresponding hub height value u_H and the wind speed u at the desired position. The 3DSL model is generally valid starting from a downstream distance where the pressure gradient in the stream-wise direction is negligible. Moreover, the viscous term is not considered and no external forces are applied.

Differently from other existing shear layer models, ~~the~~ our 3DSL approach is not formulated in a polar coordinate system, but considering a Cartesian frame of reference, i.e. the stream-wise deficit u_D, the cross-stream and vertical wind components v and w are defined along the downstream x, lateral y and upward z axis respectively. In the same way as u_D, also the two latter wind components are normalised by u_H.

Considering a dimensional analysis (Cebeci and Cousteix, 2005) the steady RANS equation for flows with a shear layer along the cross-stream and vertical component can be simplified to

$$\begin{cases} \frac{\partial u_D}{\partial x} + \frac{\partial v}{\partial y} + \frac{\partial w}{\partial z} &= 0 \\ u_D \frac{\partial u_D}{\partial x} + v \frac{\partial u_D}{\partial y} + w \frac{\partial u_D}{\partial z} &= -\left(\frac{\partial \overline{u'v'}}{\partial y} + \frac{\partial \overline{u'w'}}{\partial z} \right) \\ \frac{\partial p}{\partial y} = \frac{\partial p}{\partial z} &= 0 \end{cases} \tag{2}$$

The shear stress terms on the right hand side of the second line of Eq. (2) can be modelled by means of an eddy viscosity closure introducing the eddy viscosities ϵ_y, ϵ_z and multiplying them by the corresponding cross-stream and vertical gradients

of ~~u~~u_D:

$$\begin{aligned} \overline{u'v'} &= -\epsilon_y \frac{\partial u_D}{\partial y} \\ \overline{u'w'} &= -\epsilon_z \frac{\partial u_D}{\partial z} \end{aligned} \tag{3}$$

Further details on the eddy viscosity model are provided in Sect. 2.4.

At this point, the system of Eq. (2) is still ~~underdetermined~~under-determinated. To balance the unknown variables and the equations, we assume that the wind components v and w define a conservative vector field in all the cross-sections $y-z$. A potential function Φ can therefore be defined such that

$$\begin{cases} \frac{\partial \Phi}{\partial y} &= v \\ \frac{\partial \Phi}{\partial z} &= w \end{cases} \tag{4}$$

Concerning multiple wakes, this assumption does not imply any limitation since ~~the~~ a vector field resulting from the superposition of conservative vector fields is still conservative. However, this assumption limits the domain of possible solutions. For instance, swirling wakes in which the tangential velocity is inversely proportional to the distance from the rotation axis are accepted, while wakes rotating as a rigid body are not.

The hypothesis of a potential flow is implicit in the axial symmetry imposed by Ainslie. ~~His model~~In his model, he considers a cylindrical coordinate system defined by the radial coordinate r, the angular coordinate θ and the ~~horizontal~~ axial coordinate x. The corresponding velocity vector field $\overline{V}(r,\theta,x) = (v_r, v_\theta, u)$ is conservative only if $\nabla \times \overline{V} = 0$. Considering the individual cross-section planes at a certain x coordinate, it implies that $\partial v_r/\partial\theta - \partial v_\theta/\partial r = 0$. This equation is always satisfied by the Ainslie model in which the tangential velocity v_θ is neglected and the radial velocity v_r ~~is the same at each radius~~ does not vary along the angular coordinate θ when a constant radial distance r is considered.

The above explanation shows that, as the 3DSL model, also the Ainslie model assumes a potential flow and therefore no vorticity on the cross-sections $y-z$. In the vortex cylinder model of the actuator disk (Burton et al., 2011), the flow field of a wind turbine wake is conservative everywhere but on the surface of the vortex cylinder which enclose the wake, along the root vortex and on the bound vortex sheet swept by the rotor blades. Accordingly, our approximation to a potential flow is reasonable for most of the simulation domain and, even if the real flow is not strictly conservative, the 3DSL model enables to find one of the solutions for the underdetermined, three dimensional shear layer problem that respects the conservation of mass and the momentum balance in the streamwise direction.

Thanks to Eq. (4) and considering that ~~$\partial u/\partial x$~~ at each individual vertical cross-section $\partial u_D/\partial x$ depends only on y and z~~at each vertical cross-section~~, the conservation of mass (Eq. (2), first line) can be expressed as

$$\frac{\partial^2 \Phi}{\partial y^2} + \frac{\partial^2 \Phi}{\partial z^2} = g(y,z) - g \tag{5}$$

where ~~$g(y,z) = -\partial u_D/\partial x$~~ $g(y,z) = \partial u_D/\partial x$. This formulation is a second order elliptic partial differential equation of the Poisson type, which can be solved numerically.

Considering the aforementioned assumptions, the final formulation of the 3DSL model can be summarised as

$$\begin{cases} \frac{\partial^2 \Phi}{\partial y^2} + \frac{\partial^2 \Phi}{\partial z^2} &= -g \\ g &= \frac{\partial u_D}{\partial x} \\ \frac{\partial \Phi}{\partial y} &= v \\ \frac{\partial \Phi}{\partial z} &= w \\ u_D \frac{\partial u_D}{\partial x} + v \frac{\partial u_D}{\partial y} + w \frac{\partial u_D}{\partial z} &= \epsilon_y \frac{\partial^2 u_D}{\partial y^2} + \epsilon_z \frac{\partial^2 u_D}{\partial z^2} \end{cases} \tag{6}$$

2.2 The numerical implementation

The 3DSL model is implemented using finite difference schemes to obtain the numerical formulation of the physical model defined in Eq. (6). ~~On the vertical~~ Stream-wise gradients are approximated with a forward finite difference scheme, while a central one is used for the gradient in the other directions. The solution of the wind field on each consecutive cross-section is accomplished with the following steps:

1. Approximation of the stream-wise gradient $g = \partial u_D / \partial x$ from the stream-wise momentum balance (Eq. (6), fifth line) evaluated on the previous cross-section.
2. Computation of the potential function Φ on the previous cross-section solving the Poisson equation (Eq. (6), first line)
3. Correction of v and w on the previous cross-section with the values derived from definition of Φ (Eq. (6), third and forth lines).
4. Re-iteration of the cycle from step 2 until sufficient convergence of v and w is reached.
5. Evaluation of u_D on the current section by means of numerical integration of Eq. (6, second line).

For the initial condition on the first cross-section, a disc actuator model can be applied to estimate u_D, while v and w are set to zero.

The vertical cross-sections ~~$y-z$, the grid points are equally spaced, while the downstream stepsize~~ $y-z$ are defined by a regular grid with spacing $\Delta y = \Delta z = h$; the resolution Δx along the x axis is evaluated at each cross-section. This is needed to accomplish the stability constraints of the numerical solution. In fact, the stream-wise momentum balance (Eq. (6, fifth line) is similar to the much simpler problem

$$\frac{\partial \zeta(y,z,t)}{\partial t} = \left(\frac{\partial^2 \zeta(y,z,t)}{\partial y^2} + \frac{\partial^2 \zeta(y,z,t)}{\partial z^2} \right) \mu. \tag{7}$$

The ~~numerical problem can be solved iteratively for well defined initial and boundary conditions. The former are evaluated using a near wake model to calculate~~ solution of this problem with a so called forward-time central-space (FTCS) finite difference scheme is numerically stable only if $\mu \Delta t / h^2 \leq \frac{1}{4}$, where Δt and $h = \Delta y = \Delta z$ are the time and space discretisation

increments respectively. Inspired by this constraint, we conservatively defined the downstream step size at each cross-section as

$$\Delta x = \frac{\min(u_D)\, h^2}{4 \max(\epsilon_{y,z})} \tag{8}$$

.

The boundary conditions are assigned in two different ways: periodic conditions are applied to solve the Poisson equation (Eq. (6), first line), while, for the solution of the stream-wise ~~deficit at the~~ momentum balance (Eq. (6), fifth line), u_D is set as in the initial conditions on the boundaries.

2.3 The model initialization

To run simulations with tge 3DSL model it is necessary to initialise it with the wind field at the downstream outlet of the induction zone of the rotor, i.e. ~~where the stream-wise pressure gradient is negligible. The latter are assigned in two different ways: Periodic boundary conditions are applied~~ the region where the pressure field is influenced by the operation of the wind turbine. In fact, as explained in Sect. 2.1 the 3DSL model is not valid in the near field behind the rotor where the pressure gradients have a major influence on the flow.

Werle (2015) and Madsen et al. (2010) suggested possible methodologies suitable for this purpose. Here, we apply a classic disk actuator approach (Burton et al., 2011) to estimate the initial wake deficit $u_{D,o}$ at the outlet of the induction zone.

We consider the stream tube depicted in Fig. 2 and defined by the cross-sections at the inlet, at the rotor and at the outlet of the induction zone. We indicate the corresponding diameters as D_i, D_r and D_o respectively. We use the same subscripts for the section averaged wind speed U_{SA} and for the stream-wise wind component u. Following the disk actuator theory, we assume that:

- U_{SA} is homogeneous on each cross-section of the stream tube.
- The induction factor a defined by the thrust coefficient C_T as in Eq. (16) regulates the evolution of U_{SA} through the stream tube such that

$$a = 1 - \frac{U_{SA,r}}{U_{SA,i}} = \frac{1}{2}\left(1 - \frac{U_{SA,o}}{U_{SA,i}}\right) \tag{9}$$

According to the conservation of mass of an incompressible flow across the stream tube (see Fig. 2), the following equivalences apply:

$$U_{SA,i}\, D_i^2 = U_{SA,r}\, D_r^2 = U_{SA,o}\, D_o^2 \tag{10}$$

Replacing the induction factor in Eq. (10), it is possible to calculate the inlet and the outlet cross-section diameters of the stream tube:

$$\begin{aligned} D_i &= D_r \sqrt{(1-a)} \\ D_o &= D_r \sqrt{\tfrac{(1-a)}{(1-2a)}} = D_i \sqrt{1-2a} \end{aligned} \tag{11}$$

The initial conditions $u_{D,o}$ for the ~~solution of the Poisson equation (~~3DSL model are calculated in three steps: First, the induction factor a is homogeneously applied to the inflow wind speed u_i on the inlet cross-section of the stream tube.

$$\begin{cases} u_o = u_i\,(1-2a) & \text{on the inlet cross section} \\ u_o = u_i & \text{outside the inlet cross section} \end{cases} \tag{12}$$

Then, the wind field is expanded according to Eq. (~~6), first line)on the lateral, top and bottom boundaries of the computational domain. Differently, for the stream-wise momentum balance (~~11). Finally, the initial deficit $u_{D,o}$ is given replacing u by u_o in Eq. (1).

To calculate the stream tube cross-sections and the corresponding average wind speeds, this method needs to be applied iteratively until convergence. In fact, the induction factor a has to be known. Usually, it can be derived from the thrust coefficient C_T associated to the undisturbed wind speed at the inlet of the stream tube according to the wind turbine specification. In the case described here, the undisturbed wind speed is defined as average over the inlet cross-section by $U_{SA,i}$, which in turn is dependent on the induction factor a (see Eq. (~~6, fifth line)u_D is set as in the initial conditions on the same boundaries. Furthermore, the ground effects are reproduced by imposing $\partial\Phi/\partial z = 0$ on the lower boundary of the domain.~~ 11)). For this reason, an iterative process is applied starting with the rotor diameter D_r as first guess to approximate the diameter D_i of the inlet cross-section.

As already mentioned several times, shear layer wake models are valid only outside the induction zone. However, Madsen et al. (2010) no that the turbulent mixing influences the wind deficit profile already within this region. Therefore, they simulated wakes with their shear layer model starting from the rotor position. To compensate for the effect of pressure gradients not included in their model, but actually present in the reality until 2-3 rotor diameter downstream the turbine, they apply a linear filter to the ambient eddy viscosity within this range. In the same way, also the 3DSL model evaluates first the wind deficit outside the induction zone to initialise the wake simulation, which in turn starts directly behind the rotor. Then, it applies the linear filter

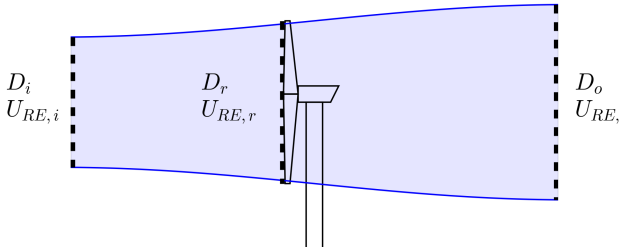

Figure 2. Sketch of the stream tube used to describe the disc actuator approach. The dashed lines represent the inflow, rotor and outlet cross-section which are indicated with the subscripts i, r, and o in the definition of the diameter and D and the section average wind speed U_{SA}.

F_2 defined in Eq. (13) to the ambient eddy viscosity to mimic the effects of the pressure gradients within the near wake.

$$\begin{cases} F_2 = \frac{x/D_r}{2.5} & \text{for } 0 < x \leq 2.5D_r \\ F_2 = 1 & \text{for } x > 2.5D_r \end{cases} \tag{13}$$

2.4 Eddy viscosity model

In the 3DSL model, the eddy viscosity is evaluated as

$$\epsilon_{y,z}(x,y,z) = \frac{F(x)\,k\,r_{y,z}(x)\,u_{a\,y,z}(x)}{\Phi_m(z_H/L_{MO})} \frac{F_1(x)\,k\,r_{y,z}(x)\,u_{a\,y,z}(x,y,z)}{\Phi_m(z/L_{MO})} + \kappa\,u_*\,z_H \frac{F_2(x)\kappa\,u_*\,z}{\Phi_m(z/L_{MO})} \tag{14}$$

following the approach suggested by ~~Lange et al. (2003) who combines~~ Ainslie (1988) who combined the contribution of the wake (first addend) and of the atmosphere (second addend).

In Eq.14 we indicate the spatial dependence of the parameters, because we want to stress the fact that, thanks to the three-dimensions resolved by the model, also the eddy viscosity does not need to be axisymmetric anymore and can be defined locally. For instance, it can vary linearly over the height z or depend on the local strain rates of the wind field as Sect. 2.4.1 will explain.

The parameters describing the wake contribution to the eddy viscosity are the empirical parameter $k = 0.015$ and the filter function[1]

$$F(x)_1 = \begin{cases} 0.65 + \left[\left(\frac{x/D_r - 4.5}{23.32}\right)^{1/3}\right] & 0 < x \leq 5.5\,D_r \\ 1 & x > 5.5\,D \end{cases} \tag{15}$$

which are included to modulate the development of the turbulence generated by the shear layer within the wake deficit (Ainslie, 1988). Last, the parameters ~~$r_{y,z}(x)$ and $u_{a\,y,z}(x)$~~ $r_{y,z}$ and $u_{a\,y,z}$ are meant to represent the characteristic length and velocity ~~turbulence scales of the wake deficit~~scales of turbulent fluctuations within the wake.

The parameters appearing in Eq. (14) to model the effect of the atmospheric conditions on the eddy viscosity are the momentum flux profile $\Phi_m(z_H/L_{MO})$ as function of the wind turbine hub height z_H and of the Monin-Obukonov length L_{MO} (Dyer, 1974), the Von Karman constant κ and the friction velocity u_*. ~~In a neutrally stratified atmosphere, u_* is proportional to the standard deviation of the stream-wise wind velocity (Panofsky and Dutton, 1984). Referring to experimental data (Panofsky and Dutton, 1984; Lange, 2002), it can be approximated with~~

As explained in Sect. 2.3, the filter function F_2 was added following the example by Madsen et al. (2010) to compensate for the pressure effect within the near wake when the 3DSL model is initialised at the rotor position.

$$u_* = \frac{u_{H_{std}}}{2.4} = \frac{TI\,u_H}{2.4}$$

~~where u_H, $u_{H_{std}}$ and TI are the inflow velocity at hub height, its standard deviation and the corresponding ambient turbulence intensity.~~

[1] in Eq. 14 the rational exponent 1/3 indicates the real cube root of the corresponding base

2.5 ~~Wake characteristic turbulence scales~~

2.4.1 Characteristic scales of turbulent fluctuations within wakes

In the 3DSL model, the ~~representative wake deficit radii in the y and z directions are regarded as the~~ characteristic turbulence length scales r_y and r_z ~~in the corresponding directions. To evaluate r_y and r_z, we average all the values of the wake deficit corresponding to the same y or z respectively. Then, we define the wake width in the y and z directions as the cumulative width where the wake deficit is below 0.1 . Finally, we consider the radius r_y (r_z) as half of~~ are both approximated with a representative wake deficit radius $r(x)$ derived as a function of the normalised downstream distance x and the ~~resulting width~~thrust coefficient C_T using the analytical wake model by Frandsen et al. (2006) and revised by Rathmann et al. (2006).

$$\begin{aligned} r(x) &= [\max(\beta, 0.7\,x/D_r)]^{0.5} && \text{where} \\ \beta &= \tfrac{1-a}{1-2a} && \text{and} \\ a &= \tfrac{1-\sqrt{1-C_T}}{2} \end{aligned} \tag{16}$$

In case of multiple wakes, only the turbine closest to the considered cross-section is regarded in the evaluation of $r(x)$ within the overlapping area.

On each cross-section, we define ~~a~~ the local characteristic turbulence velocity scale $u_{a\,y,z}$ as a function of the position $P = (x, y, z)$. For this purpose, the local characteristic velocity scale is derived with the classic turbulence mixing length theory (Pope, 2000), similarly as in the model by Keck et al. (2012). Accordingly, the turbulent velocity scales are modelled by means of the local strain rates of the wake deficit $u'_y(P) = \frac{\partial u}{\partial y}\Big|_P$ and $u'_z(P) = \frac{\partial u}{\partial z}\Big|_P$ together with the turbulence length scale ~~$r_{y,z}(x)$~~ approximated with $r(x)$ in the considered direction:

$$u_{a\,y,z}(P) = u'_{y,z}(P)\, r_{y,z}(x) \tag{17}$$

~~Finally we introduce the eddy viscosity factor~~

$$f_{y,z}(x) = F(x)\, r^2_{y,z}(x)$$

~~which will be useful in the discussion of the results and allows to rewrite Eq. (14) as~~

$$\epsilon_{y,z}(P) = \frac{k\, f_{y,z}(x)\, u'_{y,z}(P)}{\Phi_m(z_H/L_{MO})} + \kappa\, u_*\, z_H$$

2.5 ~~The near wake initialization~~

~~To run 3DSL model simulation it is necessary to initialise it with the wind field outside the induction zone of the rotor, because the 3DSL model is not valid directly in the near field behind the rotor as explained in Sect. 2.1.~~

~~Werle (2015) and Madsen et al. (2010) suggested possible methodologies suitable for this purpose. Here, we apply a classic disk actuator approach (Burton et al., 2011). We consider a stream tube defined by the cross-sections in the inflow, at the rotor~~

and at the outlet of the induction zone. We indicate the corresponding diameters as D_i, D_r and D_o respectively and we use the same notation for the rotor equivalent wind speed (REWS) U_{RE} (i.e. the average wind speed on the rotor plane) and the stream-wise wind component u. The induction factor a is derived from the evolution of U_{RE} across the stream tube as

$$a = 1 - \frac{U_{RE,r}}{U_{RE,i}} = \frac{1}{2}\left(1 - \frac{U_{RE,o}}{U_{RE,i}}\right)$$

In the calculation of the near wake, first we apply an iterative process to estimate $U_{RE,i}$ until the convergence of D_i: We calculate $U_{RE,i}$ averaging the wind speed u_i on the inflow cross-section D_i. For the first iteration D_i is approximated to the rotor diameter D_r. From the thrust coefficient C_T corresponding to $U_{RE,i}$ we calculate the induction factor

$$a = \frac{1}{2}\left(1 - \sqrt{1 - C_T}\right)$$

and we use it together with the conservation of the mass flow within the stream tube to calculate the new estimation of D_i:

$$D_i = D_r\sqrt{(1-a)}$$

A new $U_{RE,i}$ is then calculated from the new D_i at each iteration step. Once the convergence is reached, the corresponding induction factor is applied to u_i on the inflow cross-section which is then expanded to match the outlet cross-section applying the conservation of mass to the stream lines within the stream tube

$$\begin{aligned} u_o &= u_i\,(1-2a) \\ D_o &= D_r\frac{\sqrt{(1-a)}}{\sqrt{(1-2a)}} \end{aligned}$$

Finally the initial deficit u_{nw} at the near wake outlet is given replacing u_w by u_o in Eq. 1.

Sketch of the stream tube used to describe the disc actuator approach. The dashed lines represent the inflow, rotor and outlet cross-section which are indicated with the subscripts $_i$, $_r$, and $_o$ in the definition of the diameter and D and the rotor equivalent wind speed U_{RE}.

2.5 Multiple wakes

The 3DSL model is meant to improve the simulation of wakes interacting in a wind farm replacing the superposition methods usually applied (e.g. the linear or squared addition) by the simulation of all the wakes at once based on a less approximated physical model.

In practice, a wind farm simulation with the suited for simulation of multiple wakes and does not require the addition of individual wake to resolve the wind field where wakes from different turbines are overlapping. Still, for the simulations of multiple wakes it has to deal with the definition of the inflow wind field of a wind turbine hit by other wakes. This is a delicate matter because it generates a sort of conflict between the actuator disc model used for the initialisation of the 3DSL model is divided in blocks, each one dealing with the area within two rows of wind turbines perpendicular to the wind direction, or

with the wake of the whole wind farm in case of the last block. The simulation of the first block starts with the evaluation of the wakesoutside the induction zone of the turbines in the first row using the near wake model of Sect. 2.3 and stops when the second row of turbines is reached. The simulation of the next block begins with the application of model and the recovery of the wake within the near wake model to the last wind field cross-section of the previous block. The simulations within the blocks are run on the local stream-wise coordinate x_b, which measures the downstream distance from the beginning of the considered block.

upstream induction zone of the downstream turbine.

In the application of the near wake model within a wind farm, i.e. downstream the first row of turbines, we consider the wind field on the rotor cross-section as the inflow in the evaluation of the REWS. Doing this we neglect the effect of the induction zone upstream the wind turbine, but this is necessary in order to consider the recovery of the wake. The induction zone, that is the region affected by directly affected by the pressure gradients across the rotor, begins already in the inflow. For instance the IEC 61400-12-1 standard for power performance measurements suggests to measure the wind speed of the free inflow 2.5 at least 2 rotor diameters upstream the wind turbine. Power performance measurements exclude the case of wind turbine operating in wakes. We could have followed this indication anyway, but we would have disregard would have disregarded the recovery of the wake. This issue could be solved by recent

When a wind turbine operates within a wake, the 3DSL model uses the wind field on the rotor cross-section as the inflow in the evaluation of the section average wind speed $U_{SA,i}$. Doing this it neglects the effect of the induction zone upstream of the wind turbine, but this is necessary in order to consider the recovery of the wake. Recent studies which investigate how to model the induction zone in upstream upstream of the wind turbine rotor (Forsting et al., 2016) could provide tools to improve this pragmatic approach, but it is out of the scope of this work. the present work.

3 Model assessmentWake simulations

An evaluation of the 3DSL model is presented in this section , first with regards to the Ainslie model applied to an axisymmetric wake. The 3DSL model is then applied for the simulation of multiple wakes and is assessed using a LES as reference. In the former case the radius and the center-line value of the wake deficit were used as figures of merit. In the latter case, we compared the direct simulation of the interacting wakes by means of the 3DSL model as described in Sect. 2.5 with the quadratic addition of three individual wakes. In this regard, we used the REWS as term of comparison.

3.1 Model verification on single wakes

To check the consistency of the In this section we consider single and multiple wind turbine wakes from LES wind fields as reference to evaluate and compare results from simulations carried out with the 3DSL model with the axisymmetric models, we studied six test cases in which we compared the 3DSL model against the Ainslie model and with the Ainslie model as implemented in the wind farm layout software *FLaP* (Lange et al., 2003). In this regard, we decided to adopt for both models the near wake model implemented in *FLaP* to initialise the simulations.

3.0.1 The test case

The test cases deal with axisymmetric single wakesof an NREL offshore 5-MW baseline wind turbine (hub height z_H and rotor diameter D of 80 m and 126 m respectively) defined by Jonkman et al. (2009) operating in different atmospheric conditions: A neutral atmospheric stratification, i.e. $\Phi_m(z_H/L_{MO}) = 0$ with three different values of turbulence intensity (TI: 5%, 10% and 15%). For each case, two different hub height inflow conditions (u_H: 8 m/s and 15 m/s) were simulated. The corresponding thrust coefficients (C_T: 0.776, 0.256) were adopted to evaluate the initial wake deficit u_0 $2D$ downstream the rotor (Lange et al., 2003):

$$
\begin{aligned}
u_0 &= 1 - u_{0_{c-l}} \exp\left(-3.56\left(\tfrac{y}{r^*}\right)^2\right) && \text{where} \\
r^* &= \left(3.56 \tfrac{C_T}{4u_{0_{c-l}}\left(1-0.5u_{0_{c-l}}\right)}\right)^{\frac{1}{2}} && \text{and} \\
u_{0_{c-l}} &= C_T - 0.05 - (16C_T - 0.5)\,0.1\,\tfrac{TI}{100}
\end{aligned}
$$

3.0.1 Simulations and results

We evaluated the wake deficit on a 10 D long domain with a 5 D x 5 D cross-section. We used a fixed downstream incremental step in the *FLaP* simulations, providing 17 downstream positions x. Differently, the 3DSL model implements a dynamic step size to ensure the numerical convergence of the solution. The resulting number of downstream positions computed for each test case is listed in Table **??**.

Test cases and number of downstream positions x calculated with the 3DSL model. TI %55 1010 1515 u_H ms^{-1}8 158 158 15 C_T -0.776 0.256 0.776 0.2560.776 0.256 N. x 199 147 316 269437 392 The center-line value u_{c-l} and the corresponding radius r defined as the distance from the rotor axis at which the wake deficit has recovered to 97.17 (Lange et al., 2003) were chosen as basis for the evaluation and are addressed in Fig. **??**. The two models provided very similar results with a maximal discrepancy in the radius of about 0.08 and of about 0.2 in the center-line deficit. For the latter, an offset is accumulated until about $x = 3\,D$; afterwards it seems to converge to a constant value. The oscillation of the curves is related to the rougher discretisation of the x axis used in *FLaP*. the latter case we applied the square addition approach to multiple wakes.Accordingly, the local wake deficit resulting from the overlapping of the consecutive wakes is assumed as Differences in the downstream development of the center-line deficit (top) and wake radius (bottom) between the Ainslie and the 3DSL model.

$$
u_D = 1 - \sum_i (1 - u_{D,sw_i})^2 \tag{18}
$$

3.1 Model evaluation on interacting wakes

To evaluate the advantages provided by the 3DSL model in comparison to the squared addition of the deficits implemented for the simulation of merging wakesin axisymmetric models, we addressed a wind farm including three turbines and compared the two approaches in a benchmark. We decided to consider the case of where u_{D,sw_i} is the deficit of the i-th single wake. The

comparison includes three cases of multiple wakes (namely aligned wakes, wake-turbine and wake-wake interaction~~(Fig. 1c)in order to avoid the issue mentioned in Sect. 2.5 about the overlapping of the induction zone in front of the rotor and an upstream wake.~~

3.0.1 ~~The reference wind field~~

), preceded by a single wake simulation.

~~The reference wind field is calculated~~

3.1 The test cases and the reference wind fields

All the test cases are simulated with the same atmospheric conditions and consider wakes generated with the LES simulation model implemented in PALM (Raasch and Schröter, 2001), coupled with an actuator disc model (Calaf et al., 2010) ~~. The case analysed here reproduces three Siemens SWT-2.3~~as reference. These LES wind fields deal with wakes from the Siemens SWT-3.6-120 wind ~~turbines~~ turbine (120 m rotor diameter D, 90 m hub-height z_H). In the test cases two, three and four, the turbines are placed with a consecutive downstream displacement of 6 D ~~downstream and 1.5 D~~ and a cumulative offset in the cross-stream direction ~~as illustrated~~ of 0.0 D, 0.5 D and 1.5 D respectively. These layouts lead to the hub height maps of the wake deficit displayed in Fig. ~~??~~3.

The wind field ~~was~~ is evaluated on a uniform grid with a spacial resolution of 10 m (0.083 D) and a total domain size of approximately 20 km, 5 km and 3.5 km along the stream-wise, cross-stream and vertical axes respectively. The reference wind field results from the temporal average of 45 min ~~simulated~~ simulations with a time step close to 1 s. With a roughness length $z_0 = 0.002$ m and a vertically constant potential temperature the wind conditions should resemble a typical offshore boundary layer in neutral stratification ($\Phi_m(z_H/L_{MO}) = 1$). The ~~hub height inflow~~ friction velocity u_* evaluated fitting the logarithmic profile $u = (u_*/\kappa) ln(z/z_0)$ to the average vertical profile of the wind speed on the inflow section is about 0.3ms^{-1}. Under this conditions, the hub height wind speed 3.3 D upstream of the first rotor ~~has a wind speed of 8.26~~is 8 ms^{-1} with 5 % turbulence intensity TI.

According to this inflow wind speed, the wind turbines are operating in partial load with a thrust coefficient C_T of 0.858 (Thøgersen et al., 2011).

3.1.1 ~~3DSL simulations~~

~~We performed two sets of simulations with~~

3.2 Simulations with the shear layer models

The simulation domains of the 3DSL ~~model using the same inflow condition u_i which was linearly interpolated on a 5 (0.042 D) grid from the reference wind field at the 3.3 D upstream cross-section (see Fig. ??). The simulation domain covers 20~~and of the Ainslie model were different. In the first case the cross-sections were resolved with 111 and 81 points in the lateral and vertical

direction respectively, extended from $y = -7$ D to $y = +3$ D and were 8 ~~D in the stream-wise direction , has a cross-strem axis extended form about -7.5 D to 4.2 D and its height exceeds the rotor centre by 3 D~~D high. The adaptive step in the downstream direction lead to 2291 points from $x = 0$ D to $x = 20$ D. With this settings the simulation of three wind turbine wakes took about 11 s.

In ~~the first set of simulations, we reproduced the wake interaction as explained in Sect. 2.5. Three downstream blocks were considered , namely from~~ *FLaP* we imposed the initial condition taking into account the turbulence intensity, the thrust coefficient and the tip speed ratio of the turbine according to Lange et al. (2003). Additionally, for test case 2 ~~to~~ and test case 3, we considered the wake added turbulence following the empirical formula suggested by Hassan et al. (1992) as reported in (Burton et al., 2011).

For the simulation of a single wake with *FLaP*, 181 points were considered along the downstream direction from $x = 2$ D to $x = 20$ D; the radial coordinate counted 20000 points in the range from 0 D to 7 D. The enormous amount of points in the radial direction was dictated to achieve a convergent result with a downstream step close the one of the LES wind field. This simulation setup required a computational time of about 6 ~~D, from 8 to 12 D and from 14 to 20 D.~~

~~The second set of simulations involves actually a single run of the 3DSL model from 2 to 20 D downstream the rotor. Three copies of the wake provided as output were located according to the wind farm layout. In the region Ω where the wakes j were overlapping, the wake deficit u_{qs} was estimated with a square addition (Katic et al., 1986; Lange et al., 2003):~~

$$u_{qs} = \sqrt{\sum_{j\,in\,\Omega} u_j^2}$$

~~Cross-section of the inflow wind field extracted from the large eddy simulations and used as inflow condition for the 3DSL simulations. (a) Results of the wind farm simulations on the hub height plane. The black dots indicate the rotor center of the virtual wind turbines used in the assessment of the rotor equivalent wind speed. (b) Zoom on the near wakes on the hub height plane extracted from the large eddy simulations (LES). Results of the wind farm simulations on two downstream cross-sections, with two (left) and three (right) wakes. The black dots indicate the rotor center of the virtual wind turbines used in the assessment of the rotor equivalent wind speed.~~

3.2.1 ~~Results and discussion~~

s for a single wake.

~~The wake interaction and wake superposition simulation results extracted at hub height (~~

3.3 The results

For a quantitative assessment of the results, we considered several virtual turbines of the same type as the one used for the simulations; their rotors are centered on the black dots printed in the wind fields of Fig. 3~~a) and at the cross-sections 4 D downstream the second and third rotor (at $x = 6$ and 10 D~~ . An illustrative sketch of a row of the virtual turbine rotors is given in Fig. ~~?? left and right respectively), are qualitatively in agreement with the reference wind field simulated with the~~

~~LES; however there are some differences. The strongest wakes in the cross-sections of Fig. ??, that is the ones centered at $y = -1.5$ and $-3\,D$ in the top-left~~ 4.

With regard to the virtual turbine rotor j, the corresponding simulation grid points i and in relation to the reference streamwise wind component u_{ref}, we analysed

- The relative deviation of rotor average wind speed (RAWS):

$$\Delta_{RAWS,j} = \frac{\sum_{i=1}^{N_j} u_i}{\sum_{i=1}^{N_j} u_{ref_i}} - 1; \tag{19}$$

- The root mean square error (RMSE)

$$E_{RMS,j} = \sqrt{\frac{\sum_{i=1}^{N_j} (u_i - u_{ref_i})^2}{N_j}}; \tag{20}$$

- The linear regression of the streamwise wind components values on the grid points within the rotor area.

The first two figures were considered on the one hand for each virtual turbine individually. On the other hand, we calculated the overall values $\bar{\Delta}_{RAWS}$ and $\bar{E}_{RMS}$ averaging the absolute values $\Delta_{RAWS,j}$ for the former, and ~~top-right panels respectively, seem to be stretched and slightly rotated in the LES wind field, while this is not the case for the other two simulation approaches. We deem the near wake model to be the reason of this diversity. In fact, from a closer look at the reference wind fieldat hub height (Fig. 3a), the deformation of the wakes appears already in the near wake as an asymmetry with respect to the corresponding rotor axis. The deformation of the wake can be related to the vertical veer of the wind caused by the presence of the Coriolis force. This effect, which is quite small in the present LES, can cause large wake deformations in stable atmospheric stratification (Vollmer et al., 2016). Approaches to consider the~~ considering all virtual turbines at once in the calculation of the RMSE for the latter. These overall values are collected in Table 1.

The three methods of evaluation are related, but each has its own specific character. The rotor average wind speed is often used as parameter to evaluate the operational state of a wind turbine. In this sense, it is very close to the application field. However, it cannot give precise information about the accuracy of the simulated wind field because inaccurate previsions of the wake ~~stretching by wind veer in wake models (Gebraad et al.) are beyond the scope of this paper, but might become more and more relevant with increasing turbine sizes~~deficit could cancel out in the averaging process. The root mean square error does not suffer from this problem and can express the accuracy of the simulations with more confidence. Last, we included also the regression analysis in our study because in this way we could see how well the models are correlated to the reference in terms of the coefficient of determination R^2, and of the corresponding regression line slope A and intercept B. These statistical parameters are included in Table 1 too.

To provide more information on the intermediate results of the simulations, we included figures describing the development of the horizontal and vertical profiles of the wake deficit at different cross-sections in Annex A.

Table 1. Overall performance of the 3DSL model and *FLaP* (Ainslie model) in relation to the reference large eddy simulations wind field. Namely, the average deviation $\bar{\Delta}_{RAWS}$ of the rotor average wind speed, total root mean square error $\bar{E}_{RMS}$, the coefficient of determination R^2), the corresponding regression line slope A and intercept B are included.

		Test case 1		Test case 2		Test case 3		Test case4	
		3DSL	*FLaP*	3DSL	*FLaP*	3DSL	*FLaP*	3DSL	*FLaP*
$\bar{\Delta}_{RAWS}$	[−]	0.20	0.20	0.17	0.23	0.17	0.38	0.17	0.29
$\bar{E}_{RMS}/u_H$	[−]	0.27	0.29	0.31	0.31	0.29	0.48	0.34	0.46
R^2	[−]	0.93	0.92	0.95	0.97	0.96	0.96	0.94	0.90
A	[−]	0.83	0.79	1.02	0.85	0.95	0.72	0.86	0.77
B	[ms^{-1}]	1.31	1.57	-0.07	1.21	0.37	2.15	0.95	1.68

3.3.1 Test case 1: Single wake

In the first test case, we addressed a single wake to assess the general accuracy of the two shear layer wake models and at the same time to have a term of comparison for the simulation of multiple wakes.

~~As shown in Fig. 3 and in~~ Looking at the results of Fig. ~~??, the wake interaction and wake superposition approaches return~~ 5, the 3DSL model and *FLaP* tend to have fair and very similar results ~~. Maybe there is only a slight difference concerning the interface between merging wakes: With the wake addition approach, the wakes tend to remain separated and merge slower than in~~ with values of Δ_{RAWS} (top panels) and E_{RMS}/u_H (bottom panels) below 10 % after 6 D downstream. Higher errors occur in the preceding region, especially around the center of the rotor ($y = 0\ D$) where the rotor average wind speed is overestimated. Here, the 3DSL model seems to perform slightly better, in particular from the graphics of E_{RMS}. In the ~~reference wind field. In this respect, the wake interaction approach performs better~~far wake, starting from 12 D the profiles of Δ_{RAWS} and E_{RMS} do not vary much moving downstream.

~~(a) Relative deviation of the rotor equivalent wind speed (REWS) evaluated with the wake interaction and wake addition approaches at the reference cross-sections with respect to the reference wind field (b) Development of the eddy viscosity factor $f_{y,z}$ through the simulation blocks of the wake interaction approach. Here, the bottom and top horizontal axes define the downstream distance from the first upstream turbine (x) and the relative downstream distance within each block of simulation (x_b) respectively. Same as Fig. ?? but using a fixed turbulence mixing length ($r_{y,z}(x) = 1\ D$) in the eddy viscosity model.~~

~~The REWS introduced in Sect. 2.3 can provide a meaningful and more precise assessment~~ The difference between the results of the two ~~multiple wake simulation approaches. In fact, the REWS is a good estimation of the wind turbine operational wind speed from which the thrust acting on the rotor and the power extracted from the wind can be derived. For this analysis we placed a row of 14 virtual units of the same wind turbine type used in the simulations at $x = 10\ D$ and another row at $x = 16\ D$ (black dots in the wind maps~~ models perceived in Δ_{RAWS} and E_{RMS}/u_H is not found in the overall rotor average wind speed $\bar{\Delta}_{RAWS}$ and in the average root mean square error $\bar{E}_{RMS}/u_H$. Similarly, the results of the regression analysis are essentially the same for the two models. The corresponding scatter plots of Fig. ~~3 and of Fig. ??). We did this to~~

evaluate the wake interaction and the wake addition approaches for two and for three wakes . In the former case, the wakes at $y = -1.5\,D$ and $y = 0\,D$ are 10 D and 4 D long. In the latter, 16 D, 10 D and 4 D at $y = -3\,D$, $y = -1.5\,D$ and $y = 0\,D$ respectively6 and intercept B suggests that, in general, the two models tend to overestimate the wind speed values, i.e. to underestimate the deficit.

3.3.2 Test case 2: Multiple aligned wakes

Even though the simulation of consecutive aligned wakes with the Ainslie wake model does not require the square addition approach because the wind deficit profiles remain axisymmetric, we applied this approach to be consistent with the other test cases.

In the top panel of The main results are collected in Fig. **??**a, the deviation of the REWS $U_{RE,r}$ calculated from the reference wind field and from the wake interaction simulation at $x = 10\,D$ is always below 57, whose top panels show that *FLaP* overestimates the rotor average wind speed Δ_{RAWS}, particularly around the axis of the real turbine rotor ($y = 0$. In particular, the REWS is overestimated in the cross-section of the shortest wake (centre at about $y = -1.5\,D$), while it is underestimated in the cross-section of the longest wake (centre at about $y = 0\,D$). The simulations with the wake addition approach provided opposite results with an overall higher deviation with peaks up to 19D) where the maximum of the deviation is reached. Moving sideways, the deviation decreases gradually.

Differently, 3SDL model underestimates the rotor average wind speed around the axis of the real turbine rotor and overestimate it around the boundaries of the wakes ($y = \pm 1$ D). Also in this case, the highest absolute deviation from the reference is around the axis of the real turbines rotor.

In general, the results give the impression that the 3DSL model simulations are a little more accurate in terms of rotor average wind speed. The same conclusion is not evident in the values of the root mean square error drawn in Fig. 7 (bottom panels). Since in both figures of merit the two models have a very similar behaviour, it is hard to draw clear conclusion from the comparison.

In the bottom panel of Fig. **??**a, the figure of merit introduced in the previous paragraph refers to the performance of the two simulation approaches for a further downstream section ($x = 16\,D$)including a third wake around $y = -3\,D$. The wake addition method provides results very similar to those of the previous section for the wakes centred around $y = -3\,D$ and $y = -1.5\,D$.We also observe that the Contrarily from the previous test case, the overall statistics $\bar{\Delta}_{RAWS}$ and $\bar{E}_{RMS}/u_H$ sustain the impression suggested by Fig. 7: The former indicates that 3DSL simulations have a deviation from the reference of the REWS within the remaining wakes is lower than at the upstream sectionin average 6 percentile points lower than *FLaP*. In contrast, the latter suggests that the two models have the same accuracy in terms of overall root mean square error.

At the last downstream section ($x = 16\,D$) , while a lower The slope and the intercept from the regression analysis (Table 1) show that the 3DSL model approaches an almost perfect regression line. *FLaP* does not have such good results in these terms, but it is characterised by a lower spread of the data as indicated by the higher coefficient of determination R^2. This outcome can be explained with the different distribution of the deviation from the reference is found for the REWS corresponding to the wake interaction method within the two longest wakes, a very large overestimation (25)is observed for the shortest wake.The

degradation of these results is linked to the eddy viscosity factor $f_{x,y}$ and more specifically to turbulence length scale $r_{y,z}$. of the two models (see Fig. 8): The 3DSL model tends to underestimate the lower values of the wind speed, i.e. in the region around the axis of the real turbine rotor and to overestimate the higher ones. The resulting uneven distribution leads to an almost perfect regression line. Differently, *FLaP* mainly overestimates the wind speeds in their whole range causing a higher intercept and a lower slope of the regression line. The same arguments explain the results of Δ_{RAWS} described before.

According to the definition given in Sect. 2.4.1, $r_{y,z}$ equals the extension of the overall deficit considering all the wakes included on the selected section. When the number of turbines increases, this definition overestimates the turbulence mixing length scale and improperly speeds up diffusion process. The result is a too fast recovery of the wake and an overestimation of Considering all the results, we conclude that the two models simulate differently the wake of this test case, but they have very similar overall performance.

3.3.3 Test case 3: Multiple wakes with 0.5 D lateral separation

The simulation of multiple wakes with offset provided more pronounced differences between the two models. Concerning the rotor average wind speed plotted in the top panel of Fig. 9, the values of Δ_{RAWS} evaluated with the 3DSL simulations are contained within ± 10 % with negative peaks around the center line of the turbines at the corresponding first downstream cross-section ($x = 8$ D, $y = -0.5$ D and $x = 14$ D, $y = -1.0$ D); otherwise the 3DSL model overestimates the Δ_{RAWS}.

The wakes predicted with *FLaP* and the square addition rule overestimate almost everywhere the rotor equivalent wind speed .

The problem here is that on a certain values and are higher than in the case of the simulation with the 3DSL model. In the results from *FLaP*, we also notice that the maximal deviation of the rotor average wind speed at each cross-section an homogeneous eddy viscosity factor is used to modulate the diffusion at different distances from is higher than in test case 2 where the aligned wakes are supposed to be axisymmetric. Furthermore, it increases passing through the third turbine. On the contrary, we do not observe such behavior in the 3DSL model, where the maximum peaks of Δ_{RAWS} have a similar level as in test case 2 on all cross-sections. This difference between the two models might be due to the three dimensional, non axisymmetric character of the multiple wakes simulated in this test case, which is better reproducible by the 3DSL model.

Although from a different point of view, the results about the root mean square error (Fig. 9, bottom panel) lead to the rotor generating the wakes. From another perspective, three different values of eddy viscosity are implemented to simulate similar diffusive process at the same downstream distance from the rotor generating the wake. same observations.

This issue is well represented in Fig. **??**b which illustrates how the eddy viscosity factor evolves downstream through the three blocks of simulationsencompassing one (blue line), two (red line) and three (yellow line) wakes respectively. The evolution of the eddy viscosity factor in the wake addition approach (purple line) is included too and it is representative for the case of a single wake. The overall statistics provide a quantitative summary of the results mentioned above; in particular, the 3DSL model achieves a deviation from the reference rotor average wind speed ($\bar{\Delta}_{RAWS}$) 11 percentile points lower than *FLaP*. Considering the overall root mean square error, the spread between the two models is even more acute: In the simulations with the 3DSL model, $\bar{E}_{RMS}$ is almost 20 percentile points lower than in *FLaP* simulations.

~~The same figure also explains why only the REWS values within the wake of the third turbine are overestimated: The blue and red lines assigned to the single and double wake are relatively close around $x = 10\,D$. In this case~~The regression analysis replicates here the results of test case 2, with the difference that, for the 3DSL model simulations, the slope (A) and the intercept (B) of the ~~overestimation of the turbulence mixing length is partly compensated by the fact that the filter function slows down the diffusion process of the wakes from previous blocks of simulations because it is applied to the downstream distance x_b relative to the corresponding simulation block. This mitigating effect is not enough for the wake of the third rotor, whose line at $x = 16\,D$ is significantly more distant from the line representing the single wake (purple line).~~ regression line are not so close to their ideal values 1 and 0 respectively. In turn, the coefficient of determination R^2 is little higher indicating less scatter of the data. For the simulations with *FLaP* we observe a remarkable increase in the intercept which indicates a larger overestimation of the wind speed, that means a larger underestimation of the wake deficit.

~~To solve the above problem and at the same time to avoid a complex definition of a heterogeneous turbulence mixing length, we decided to fix $r_{y,z}(x) = 1\,D$. We ran the simulations again with this new settings. No significant changes were observed in the results from the wake addition approach . On the contrary, we got remarkable improvements from the wake interaction approach, in particular concerning the REWS within the wake of the third rotor at $x = 16\,D$. In~~

3.3.4 Test case 4: Multiple wakes with 1.5 D lateral separation

Due to the increased cross-stream separation between the three turbines considered in this test case, the ~~other cases a minor deterioration of the performances can be observed (see Fig. **??**a)~~flow seems composed by single wakes. The results presented in Fig. 9 are therefore comparable with those of test case 1, but with an amplified difference between the performance of the two models. In fact, with regard to the reference, both the deviation of the rotor average wind speed and the root mean square error evaluated for *FLaP* are clearly higher than the ones evaluated for the 3DSL model.

The corresponding overall values give a measure of this difference: both the deviation $\bar{\Delta}_{RAWS}$ of *FLaP* and the average root mean square error $\bar{E}_{RMS}/u_H$ are more than 10 percentile points larger than the ones of the 3DSL model.

The regression analysis provides results close to those of test case 1 for both models, a part from the intercept which reduced a little for the simulation with the 3DSL model, while it increased for *FLaP* simulations.

~~We provide here two possible explanation of the slightly worsening of the results: First, the fixed turbulence mixing length results from the compromise between characteristic turbulence length scales in the intermediate and in the very far wake~~

4 Discussion

In Sect.3.3, we compared two shear layer wake models with a different level of detail in the physical description of the flow. The results are not always easy to interpret because in some cases one model is accurate where the other is not and vice-versa. We dealt with this problem analysing different figures of merit which are generally in agreement. This temporarily solves the conflict between the applicative point of view of the rotor average wind speed and the more wind field oriented approach of the root mean square error.

The object of comparison was the performance of the two models in the simulation of multiple wakes. In this regard, the figures of merit are generally in favour of the 3DSL model. This is a positive outcome of our research and encourage the further development of this new model. Nonetheless, the two models provided similar results for axisymmetric wakes (test case 1 and test case 2). This points out the advantage given by the third dimension resolved by the 3DSL model. In fact, in the other test cases, i.e. when multiple wakes have a lateral offset, the additional details in the physical description of the flow implemented in the 3DSL model seem to improve the results. ~~An optimization or parametrisation of this value could possibly improve the results. Second, the filter function is still applied to the relative downstream distance within each simulation block. Figure ??b reveals that the incongruity of a homogeneous eddy viscosity factor for different wake conditions on the same~~

Despite the different performances, we found similar deficiencies in the two models. This particularly interests the flow of single wakes near to the rotor cross-section ~~is still unsolved~~as indicated by the results of test case 1 and in test case 4. Furthermore, the regression analysis and the scatter plot indicated , the tendency to overestimate the wake deficit in the same cases. The analysis of the individual wake profiles could help to understand how to deal with this issue. In many cases, possible solution could be provided by different eddy viscosity models. In this sense, the three dimensional domain of the 3DSL model offers the possibility to develop proper spatial distributions of these quantities, while the axisymmetric two dimesional models would have more limits in the accomplishment of this task.

5 Conclusions

~~This paper~~ This paper investigates the possibility to improve the simulation of multiple wakes with engineering wake models such as the commonly used Ainslie model (Ainslie, 1988) implemented for instance in the wind farm layout software *FLaP* (Lange et al., 2003). In this regard, the paper presents a new ~~non-axisymmetric~~ wake shear layer model (3DSL) that can deal with non-axisymmetric flows and is therefore suitable to ~~directly simulate interacting wakes . It demonstrates that the 3DSL model is equivalent to the commonly used Ainslie model (Ainslie, 1988) implemented for instance in the wind farmlayout software *FLaP* (Lange et al., 2003). Furthermore, this study provides a test case which shows how, in terms of rotor equivalent wind speed, the 3DSL model could provide more accurate results than simulation of single wakes combined with a square addition rule.~~ simulate multiple wakes at once. Differently, when the Ainslie model is applied in a wind farm, the flow of multiple wakes is evaluated superimposing the deficit of the individual wakes according to a linear or square addition approach. To allow the simulation of ~~interacting~~ multiple wakes without the superposition of the individual wakes, the 3DSL model abandons the ~~assumptions~~ hypothesis of an axisymmetric wake ~~implemented for example in the model~~ assumed by Ainslie (1988) and add a third dimension to the simulation domain. In order to do this, it assumes a potential flow on the vertical cross-sections.

~~The validation against the Ainslie model considered a wind turbine operating at high and low thrust, with different turbulence conditions. The wake radius and center-line deficit resulting from the simulation of the two codes are in agreement with a maximal variation of about 0.08% and 0.21% respectively.~~

~~In a benchmark against the large eddy simulations of three interacting wakes, we found that, at two selected cross-sections,~~ In a benchmark against large eddy simulations, we considered four test cases and compared wake simulations performed with *FLaP* and with the 3DSL model. The assessment was based on the average wind speed on the rotor of several fictive turbines and the corresponding root mean square error. The two models provided similar results when they simulated axisymmetric wakes, but the 3DSL model ~~could predict the rotor equivalent wind speed better than the squared addition of single wakes. Some differences from the reference wind field might be linked to the effect of the vertical veer within the atmospheric boundary layer and to the turbulent mixing. An enhanced near wake model and a more detailed description of the eddy viscosity could improve the agreement with the reference~~perfomed better in the test cases including non-axisymmetric wakes. In part, this might be one of the advantages of the third dimension included in the 3DSL model.

~~The proposed model positively passed the first tests and the results indicated the direction to follow for further improvements such that in the near future the simulations of wake interaction within~~ Since only few test cases using wakes simulated within large eddy simulations were addressed here, this results cannot be generalised. For the same reason we cannot make any statement about how these results could affect the estimation of the annual energy yield of a wind farm~~could benefit from the purely physical approach adopted~~ . Nevertheless, we are confident that the additional details in the physical description of the wake flow implemented in the 3DSL model ~~.~~

can in general offer new possibilities to improve the simulation of single and multiple wakes at an affordable computational cost.

Acknowledgements. This research was carried out in the frame of the RAVE (Research at alpha ventus) research project GW Wakes, funded by the German Federal Ministry for Economic Affairs and Energy (BMWi) based on a decision of the Parliament of the Federal Republic of Germany (grant number 0325397A). Computer resources have been partly provided by the North German Supercomputing Alliance (HLRN) and by the national research project “Parallelrechner-Cluster für CFD und WEA-Modellierung” (FKZ 0325220) funded by the Federal Ministry for Economic Affairs and Energy (BMWi). The authors further want to thank J. Schmidt and J.J. Trujillo for valuable discussions about the content of the manuscript.

References

Ainslie, J. F.: Calculating the Flowfield in the Wake of Wind Turbines, Journal of Wind Engineering and Industrial Aerodynamics, 27, 213–224, doi:10.1016/0167-6105(88)90037-2, 1988.

Burton, T., Jenkins, N., Sharpe, D., and Bossanyi, E.: Wind Energy Handbook, 2nd Edition, John Wiley & Sons, Ltd., Publication, 2011.

Calaf, M., Meneveau, C., and Meyers, J.: Large eddy simulation study of fully developed wind-turbine array boundary layers, Physics of Fluids, 22, 015 110, doi:10.1063/1.3291077, 2010.

Cebeci, T. and Cousteix, J.: Three-Dimensional Incompressible Laminar and Turbulent Flows, Springer Berlin Heidelberg, 2005.

Crespo, A., Hernández, J., and Frandsen, S.: Survey of modelling methods for wind turbine wakes and wind farms, Wind Energy, 2, 1–24, doi:10.1002/(SICI)1099-1824(199901/03)2:1<1::AID-WE16>3.0.CO;2-7, 1999.

Dyer, A.: A review of flux-profile relationships, Boundary-Layer Meteorology, 7, 363–372, doi:10.1007/BF00240838, 1974.

Forsting, M., Raul, A., Bechmann, A., and Troldborg, N.: A numerical study on the flow upstream of a wind turbine on complex terrain, Journal of Physics: Conference Series, 753, doi:10.1088/1742-6596/753/3/032041, 2016.

Frandsen, S., Barthelmie, R., Pryor, S., Rathmann, O., Larsen, S., Højstrup, J., and Thøgersen, M.: Analytical modelling of wind speed deficit in large offshore wind farms, Wind Energy, 9, 39–53, doi:10.1002/we.189, http://dx.doi.org/10.1002/we.189, 2006.

Gebraad, P. M. O., Churchfield, M. J., and Fleming, P. A.: Incorporating Atmospheric Stability Effects into the FLORIS Engineering Model of Wakes in Wind Farms, Journal of Physics: Conference Series, 753, 052 004, doi:10.1088/188/1742-6596/753/5/052004.

Hassan, U., xx, x., xx, x., xx, x., xx, x., and xx, x.: A wind tunnel investigation of the wake structure within small wind turbine farms, E/5A/CON/5113/1890, 1992.

Jonkman, J., Butterfield, S., Musial, W., and Scott, G.: Definition of a 5-MW Reference Wind Turbine for Offshore System Development, Tech. rep., National Renewable Energy Laboratory, doi:10.2172/947422, 2009.

Katic, I., Højstrup, J., and Jensen, N. O.: A simple model for cluster efficiency, in: EWEC Proc. '86, p. 407–10, http://orbit.dtu.dk/fedora/objects/orbit:66401/datastreams/file_f7da8eb2-e49c-4dc9-9ee5-72846f40ef34/content, 1986.

Keck, R.-E., Veldkamp, D., Madsen, H. A., and Larsen, G.: Implementation of a Mixing Length Turbulence Formulation into the Dynamic Wake Meandering Model, Journal of Solar Energy Engineering, 134, 021 012–021 012, doi:10.1115/1.4006038, 2012.

Lange, B.: Modelling the Marine Boundary Layer for Offshore Wind Power Utilisation, Ph.D. thesis, Carl von Ossietzky Universiät Oldenburg, 2002.

Lange, B., Waldl, H.-P., Guerrero, A. G., Heinemann, D., and Barthelmie, R. J.: Modelling of Offshore Wind Turbine Wakes with the Wind Farm Program FLaP, Wind Energy, 6, 87–104, doi:10.1002/we.84, 2003.

Lissaman, P. B. S.: Energy effectiveness of arbitrary arrays of wind turbines, Journal of Energy, 3, 323–328, doi:10.2514/3.62441, 1979.

Machefaux, E.: Multiple Turbine Wakes, Ph.D. thesis, Technical University of Denmark, 2015.

Madsen, H. A., Larsen, G. C., Larsen, T. J., Troldborg, N., and Mikkelsen, R.: Calibration and Validation of the Dynamic Wake Meandering Model for Implementation in an Aeroelastic Code, Journal of Solar Energy Engineering, 132, 041 014–041 014, doi:10.1115/1.4002555, 2010.

Panofsky, H. and Dutton, J.: Atmospheric Turbulence: Models and Methods for Engineering Applications, John Wiley & Sons Ltd, 1984.

Pope, S.: Turbulent Flows, Cambridge University Press, 2000.

Raasch, S. and Schröter, M.: PALM - A large-eddy simulation model performing on massively parallel computers, Meteorologische Zeitschrift, 10, 363–372, doi:10.1127/0941-2948/2001/0010-0363, 2001.

Rathmann, O., Barthelmie, R., and Frandsen, S.: Turbine Wake Model for Wind Resource Software, in: EWEC, https://www.researchgate.net/profile/R_Barthelmie/publication/268300272_Turbine_Wake_Model_for_Wind_Resource_Software/links/561d248208aec7945a252a37.pdf?inViewer=0&pdfJsDownload=0&origin=publication_detail, 2006.

Thøgersen, Morten, L., Sørensen, T., Nielsen, P., Grötzner, A., and Chun, S.: WIndPro/Park. Introduction to Wind Turbine Wake Modelling and Wake Generated Turbulence, EMD International A/S, 2011.

Vermeer, L, J., Sørsen, J, N., and Crespo, A.: Wind turbine wake aerodynamics, Progress in Aerospace Science, 39, 467–510, 2003.

Vollmer, L., Steinfeld, G., Heinemann, D., and Kühn, M.: Estimating the wake deflection downstream of a wind turbine in different atmospheric stabilities: an LES study, Wind Energy Science, 1, 129–141, 2016.

Walker, K., Adams, N., Gribben, B., Gellatly, B., Nygaard, N. G., Henderson, A., Marchante Jiménez, M., Schmidt, S. R., Rodriguez Ruiz, J., Paredes, D., Harrington, G., Connell, N., Peronne, O., Cordoba, M., Housley, P., Cussons, R., Håkansson, M., Knauer, A., and Maguire, E.: An evaluation of the predictive accuracy of wake effects models for offshore wind farms, Wind Energy, 19, 979–996, doi:10.1002/we.1871, 2016.

Werle, M. J.: Another engineering wake model variant for horizontal axis wind turbines, Wind Energy, pp. 279–299, doi:10.1002/we.1832, 2015.

Appendix A: Wake deficit profiles

The comparison of the 3DLS model and of *FLaP* with the reference wind field from large eddy simulations (LES) reported in this paper deals with figure of merits representative for integral results, i.e. they can hardly reveal the actual output of the two models. For this reason we show in this annex the downstream development of the wake deficit for the test cases analysed in this paper.

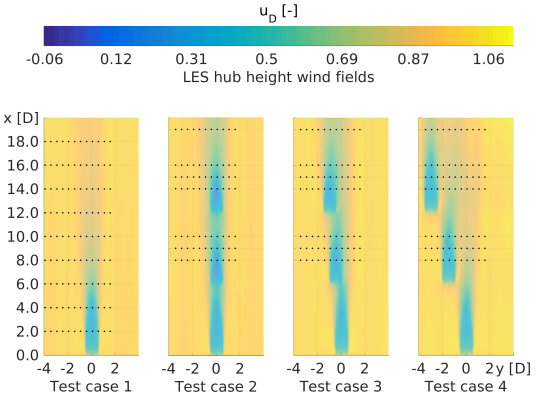

Figure 3. ~~Relative position~~ Colour map of the ~~wind turbine rotors within~~ hub height wake deficit u_D evaluated for the test cases from the large eddy ~~simulation domain~~simulations (LES).

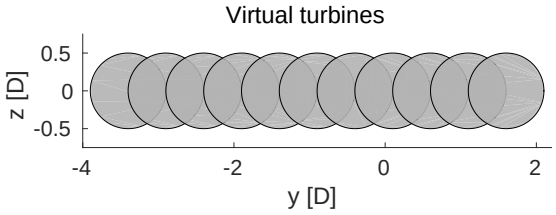

Figure 4. Illustrative sketch of the rotors of the virtual turbines considered to assess the performance of the engineering models in relation to the large eddy simulations.

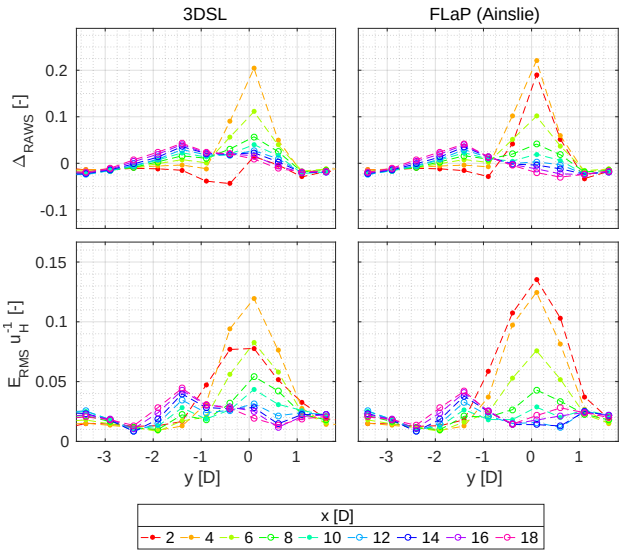

Figure 5. Test case 1 (Single wake). Deviation of the rotor average wind speed Δ_{RAWS} (top panels) and of the root mean square error E_{RMS} (bottom panels) evaluated in relation to the large eddy simulations wind field for the simulation with the 3DSL model and with *FLaP*.

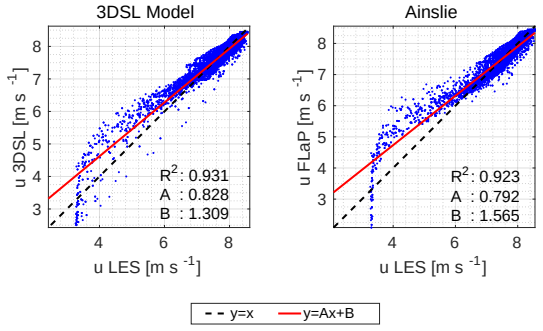

Figure 6. Test case 1 (Single wake). Scatter plot and corresponding regression line of the wind speed derived from the 3DSL model (left) and from the *FLaP* wake simulations in relation to the reference wind field calculated with large eddy simulations (LES).

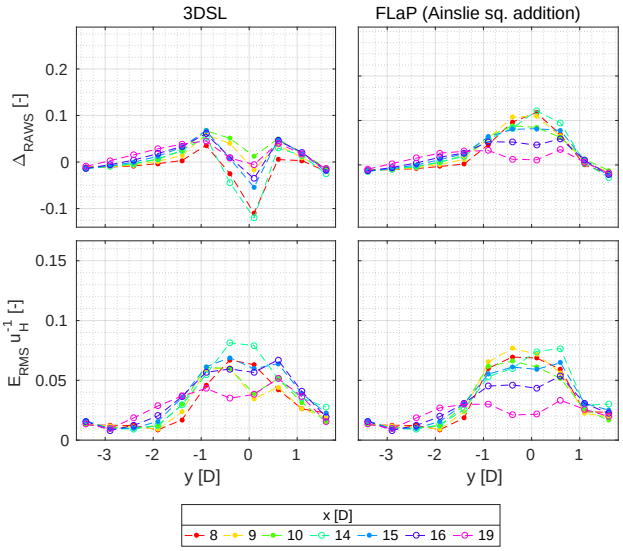

Figure 7. Test case 2 (Multiple aligned wakes). Deviation of the rotor average wind speed Δ_{RAWS} (top panels) and of the root mean square error E_{RMS}/u_H (bottom panels) evaluated in relation to the large eddy simulations wind field for the simulation with the 3DSL model and with *FLaP*.

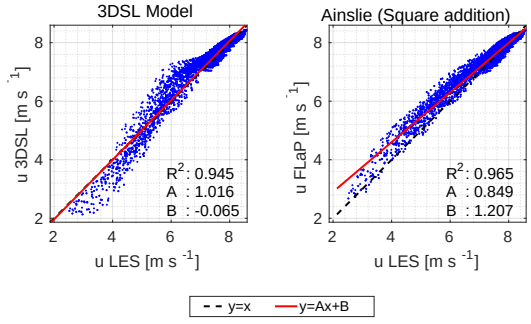

Figure 8. Test case 2 (Multiple aligned wakes) Scatter plot and corresponding regression line of the wind speed derived from the 3DSL model (left) and from the *FLaP* wake simulations in relation to the reference wind field calculated with large eddy simulations (LES).

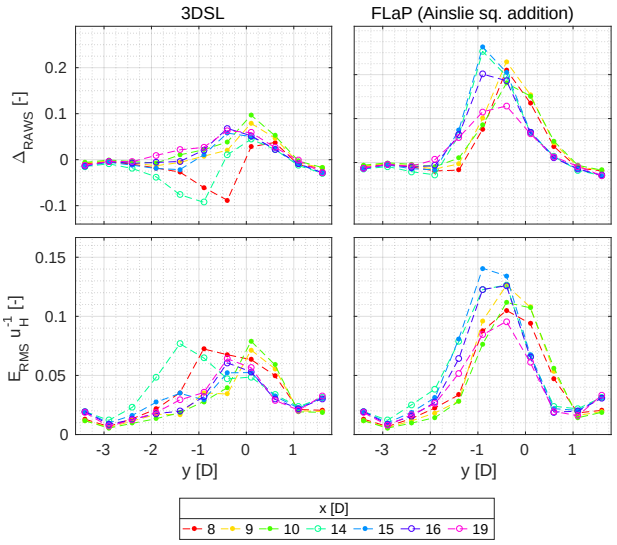

Figure 9. Test case 3 (Multiple wakes with 0.5 D later offset). Deviation of the rotor average wind speed Δ_{RAWS} (top panels) and of the root mean square error E_{RMS} (bottom panels) evaluated in relation to the large eddy simulations wind field for the simulation with the 3DSL model and with *FLaP*.

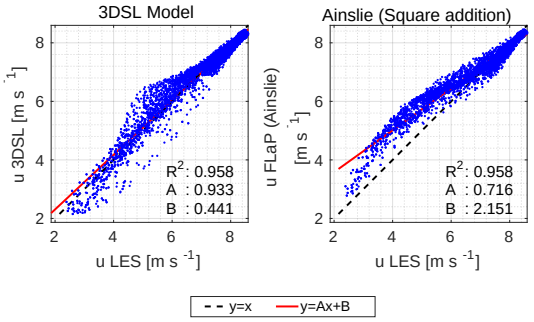

Figure 10. Test case 3 (Multiple wakes with a 0.5 D lateral separation). Scatter plot and corresponding regression line of the wind speed derived from the 3DSL model (left) and from the *FLaP* wake simulations in relation to the reference wind field calculated with large eddy simulations (LES).

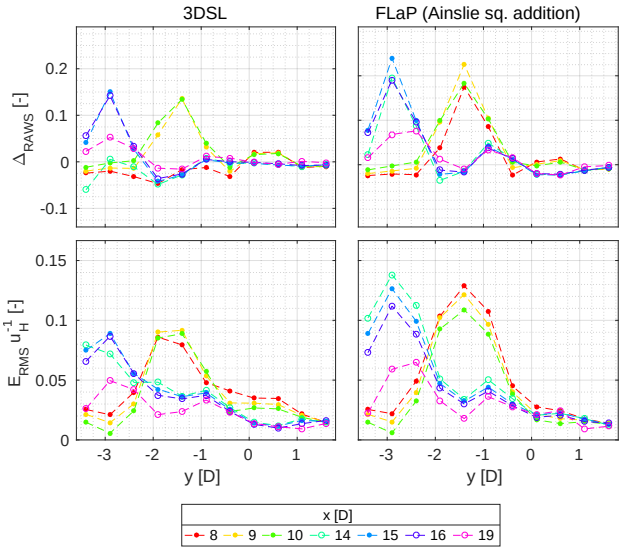

Figure 11. Test case 4 (Multiple wakes with 1.5 D later offset). Deviation of the rotor average wind speed Δ_{RAWS} (top panels) and of the root mean square error E_{RMS} (bottom panels) evaluated in relation to the large eddy simulations wind field for the simulation with the 3DSL model and with *FLaP*.

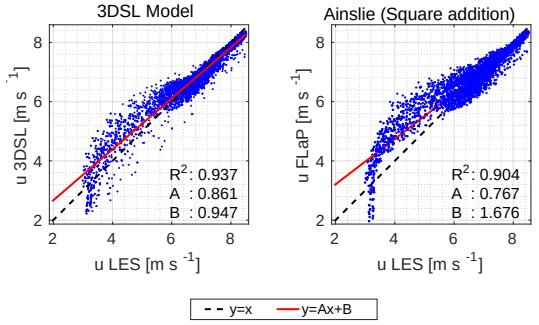

Figure 12. Test case 4 (Multiple wakes with a 1.5 D lateral separation). Scatter plot and corresponding regression line of the wind speed derived from the 3DSL model (left) and from the *FLaP* wake simulations in relation to the reference wind field calculated with large eddy simulations (LES).

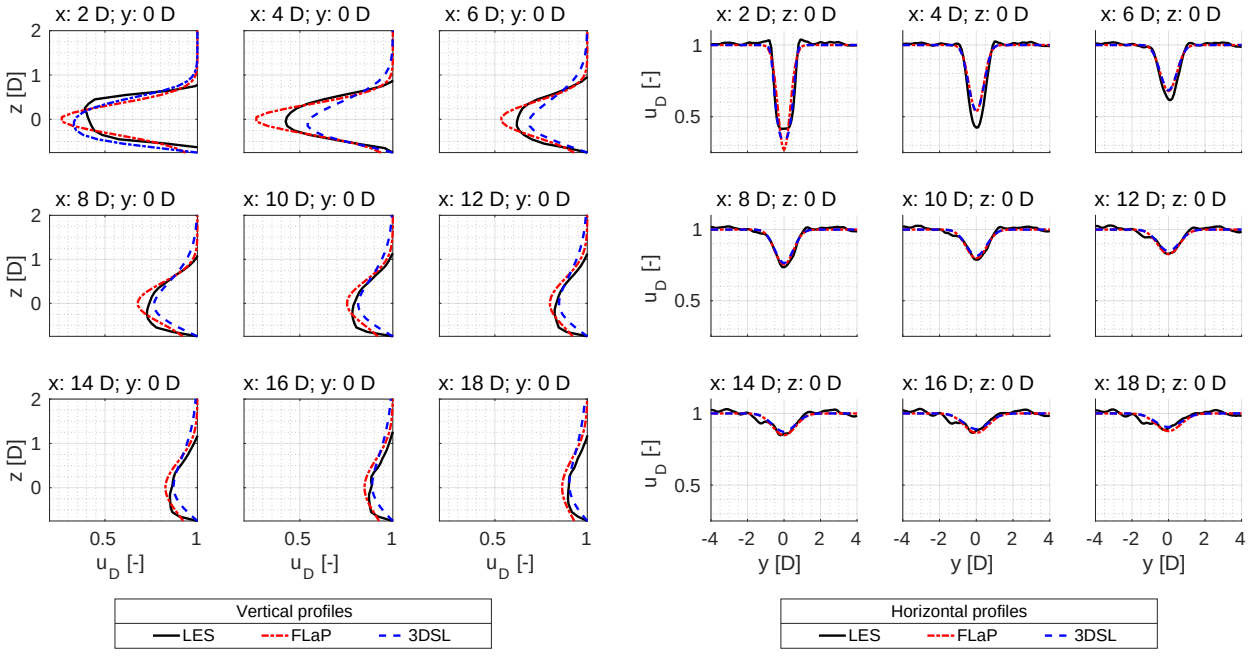

(a) (b)

Figure A1. Test case 1 (Single wake). Downstream development of the vertical (a) and horizontal (b) profiles of the wake deficit evaluated along the wind turbine rotor axis from the 3DSL model and from the *FLaP* simulations and from the reference large eddy simulation (LES) wind field.

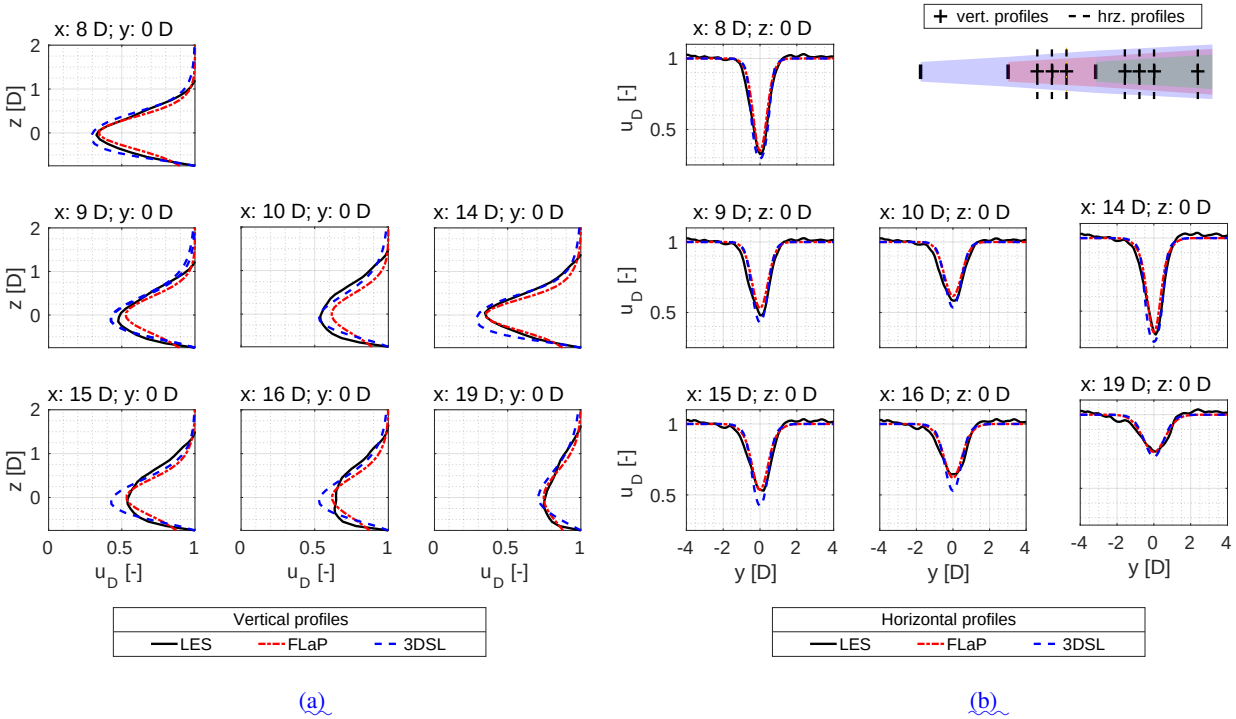

Figure A2. Test case 2 (Multiple aligned wakes) Downstream development of the vertical (a) and horizontal (b) profiles of the wake deficit evaluated along the common axis of the wind turbines from the 3DSL model and *FLaP* simulations and from the reference large eddy simulations (LES) wind field. The position of the considered profiles is illustrated in top-right corner of (b).

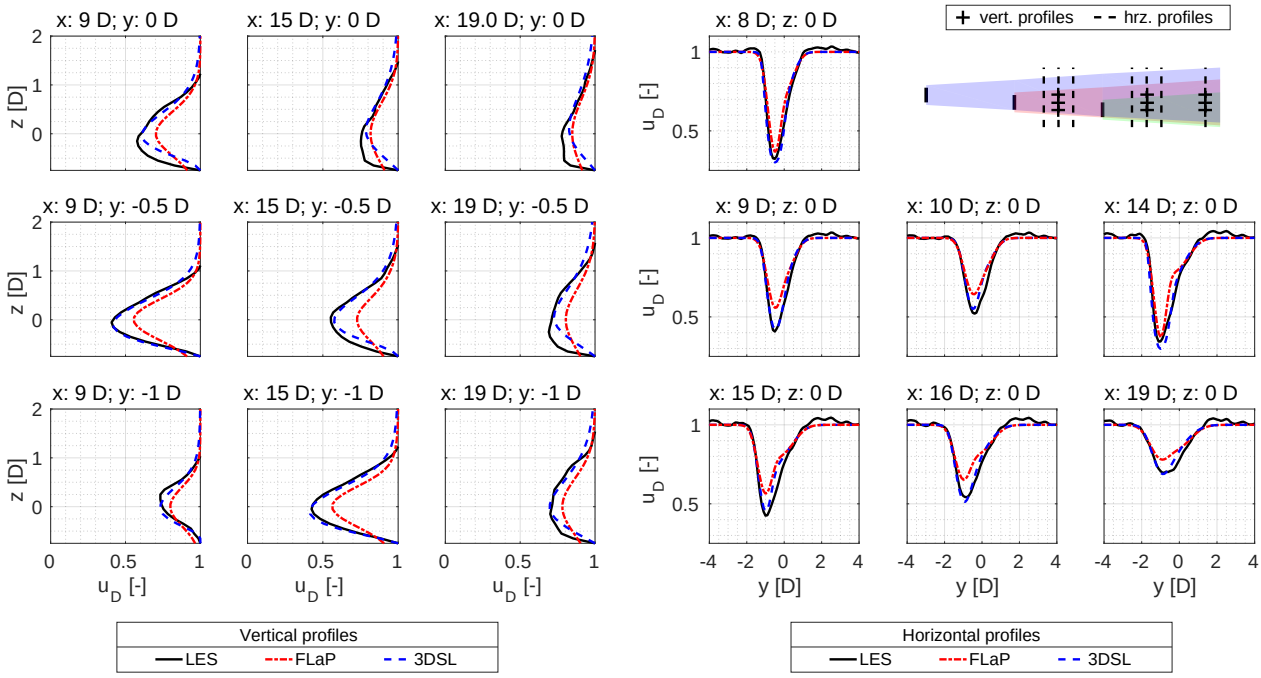

Figure A3. Test case 3 (Multiple wakes with 0.5 D lateral separation). Downstream development of the vertical (a) and horizontal (b) profiles of the wake deficit evaluated along the common axis of the wind turbines from the 3DSL model and *FLaP* simulations and from the reference large eddy simulations (LES) wind field. The position of the considered profiles is illustrated in top-right corner of (b).

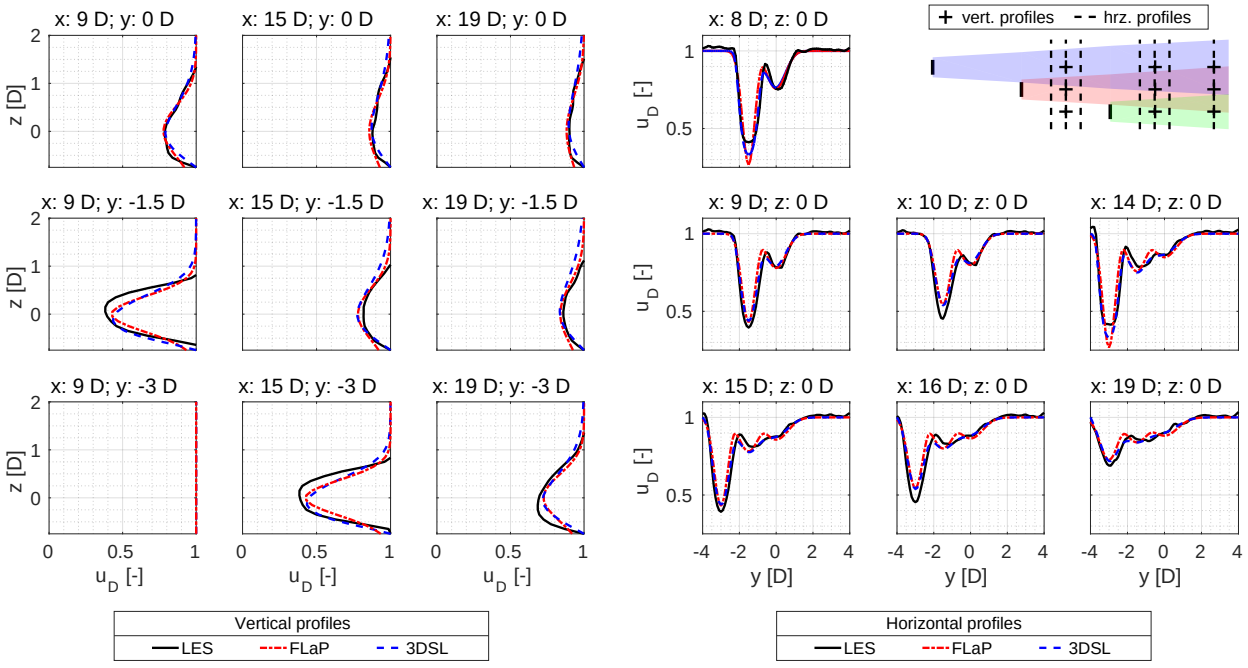

(a) (b)

Figure A4. Test case 4 (Multiple wakes with 1.5 D lateral separation). Downstream development of the vertical (a) and horizontal (b) profiles of the wake deficit evaluated along the common axis of the wind turbines from the 3DSL model and *FLaP* simulations and from the reference large eddy simulations (LES) wind field. The position of the considered profiles is illustrated in top-right corner of (b).